Mechanical and Electrical Characterization of Carbon Black-doped Closed-cell Polydimethylsiloxane (PDMS) Foam

By
Jessica A. Herring

Submitted to the
Department of Materials Science and Engineering
in Partial Fulfillment of the Requirements for the Degree of

Bachelor of Science
at the
Massachusetts Institute of Technology

June 2015

Signature redacted

Signature of Author .....
Jessica A. Herring
Department of Materials Science and Engineering
May 1, 2015

Signature redacted

Certified by .....
Jeffrey Lang
Professor of Electrical Engineering
Thesis Supervisor

Signature redacted

Certified by .....
Bilge Yildiz
Professor of Nuclear Science and Engineering and Materials Science and Engineering
Thesis Reader

Signature redacted

Accepted by .....
Geoffrey Beach
Professor of Materials Science and Engineering
Chairman, Undergraduate Thesis Committee

Table of Contents

Table of Figures

Mechanical and Electrical Characterization of Carbon Black-doped Closed-cell Polydimethylsiloxane (PDMS) Foam

Abstract

Carbon Black-doped Polydimethylsiloxane (CB-PDMS) can be used as a pressure sensing material due to its piezoresistive properties. The sensitivity of such a sensor is in part dependent on the stiffness of the material. A closed-cell CB-PDMS foam is being explored as a possible flexible, lightweight, and waterproof underwater sensing material for use in unmanned underwater vehicles and other hydrodynamic sensing purposes. The percolation threshold for conduction through the CB-PDMS foam is theorized, and a number of different concentrations based on the theorized threshold are explored in order to determine the optimum weight percent of Carbon Black dopant to achieve a high sensitivity, low stiffness sensing CB-PDMS foam. Sinusoidal mechanical pressure patterns were applied and voltage response measured. An optimum dopant weight percent out of the concentrations tested was found at 5.5 wt% CB-PDMS.

Introduction

Unmanned underwater vehicles (UUVs) are used to collect data of various kinds, such as locating underwater mine locations and shipwrecks, or mapping ocean floor topography (1). They rely on the use of sensors to navigate underwater autonomously. Most UUVs use acoustic or optical sensors to navigate (2), but these methods of undersea visualization are not energy efficient: they must send out a signal in order to read a response from the environment (3) (4), and these signals have the potential to interfere with the activity of undersea life, such as dolphins, that also use echolocation to navigate. (5) For these reasons, there is desire to design a new type of sensor for use in UUVs.

A new type of MEMS (Microelectromechanical System) sensor is proposed that does not rely on acoustic or optic signals. The proposed sensor mimics the lateral line, a biological feature of a number of species of fish. The lateral line is composed of a series of neuromasts located beneath the fish's skin. These neuromasts are connected to exterior pressures via pores in the fish's skin. Pressure differentials under the fish's pores stimulate the neuromasts, allowing the fish to sense local changes in pressure between neuromasts. These changes in water pressure are caused by vortices in the water, which are created in response to flow against an object. (6) These vortices can be analyzed to determine the location of the object giving them off. This ability to measure pressure differentials allows the fish to create a map of the area it occupies at any given time, allowing some blind species of fish, such as the Blind Cave Fish in Figure 1. (7) (13)

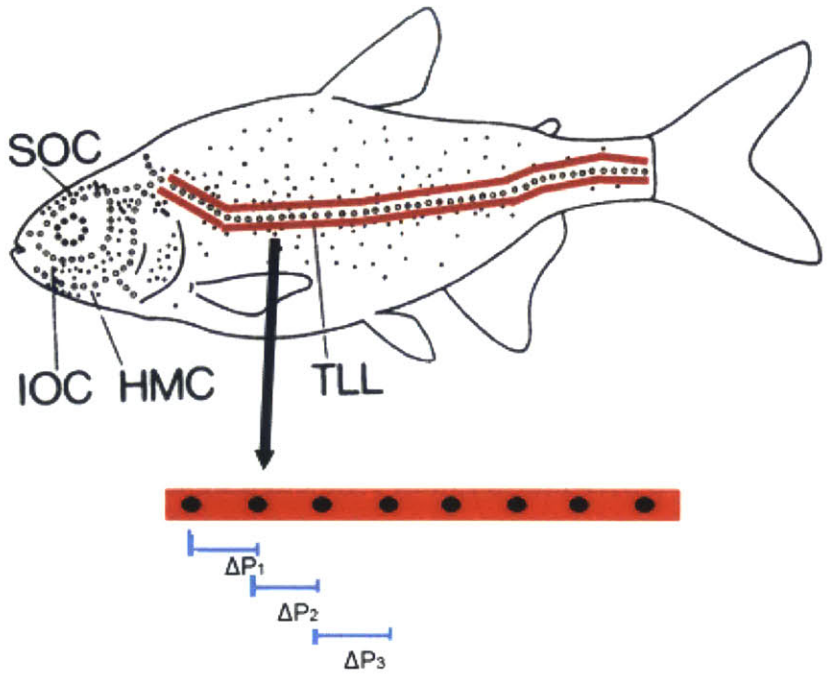

Figure 1. The lateral line of a Blind Mexican Cavefish. Neuromasts, shown as black dots, allow for the measurement of pressure differentials. Original image edited from Bleckmann (7).

This proposed sensor utilizes the conductive nature of Carbon Black (CB) and the sensitivity to small strain of a silicone elastomer, PDMS (Polydimethylsiloxane). The PDMS is used as a pliable matrix to hold the conductive particles. When the composite material is strained, it exhibits a piezoresistive response. This resulting change in electric response can be used to sense changes in pressure between different points on the sensor. These pressure differentials can be related back to hydrodynamic stimuli in the water caused by objects, allowing the sensor to determine the location of these objects by interpreting the pressure differentials along the sensor. (8)

Current designs for this sensor are shown in Figure X. Blocks of silver-doped solid CB-PDMS are used to reduce contact resistance to wires, providing ample contact area for recording piezoresistive response from the CB-PDMS foam blocks molded between. These blocks of CB-PDMS foam are held on a backing of PDMS.

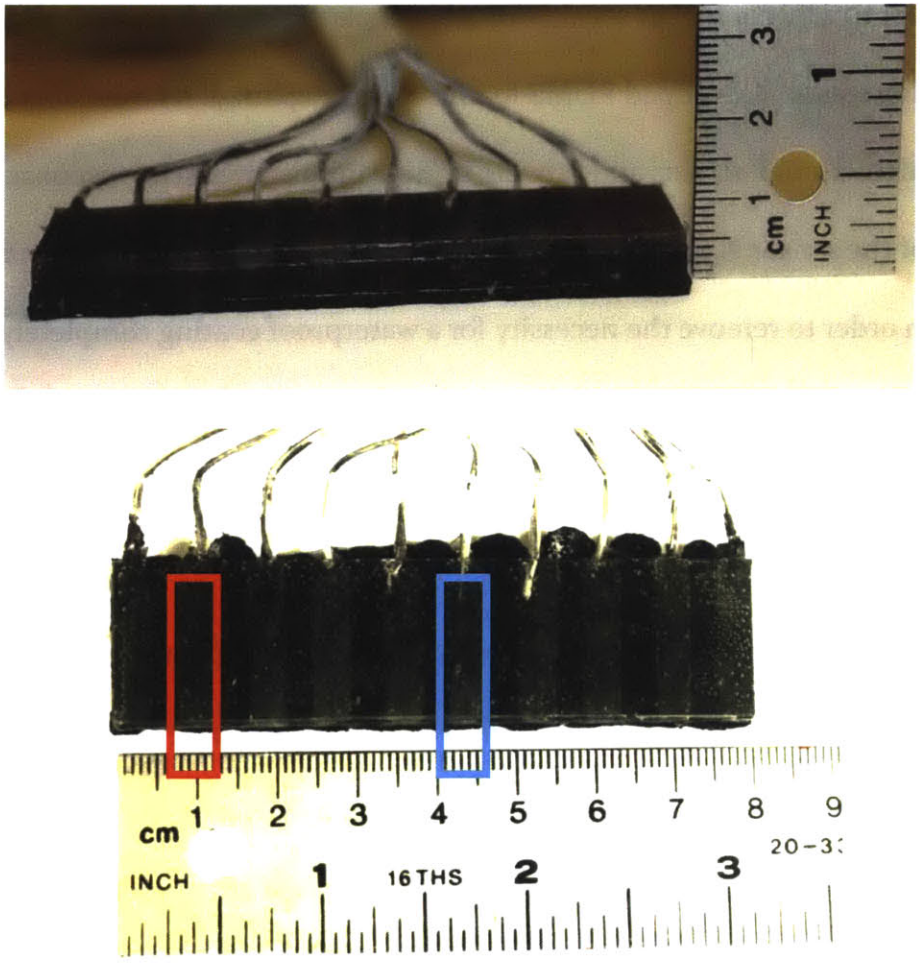

Figure 2. Array sensor made using CB-PDMS foam, solid PDMS backing, and solid Ag-CB-PDMS as electrical contacts. This sensor was designed to mimic the lateral line in fish. The red box highlights the CB-PDMS foam, while the blue highlights the solid Ag-CB-PDMS used as an electrical contact. Image credit: Jeff Dusek, 2015.

This design mimics its biological counterpart seen in the fish, allowing the flexible silicone sensor to read a number of pressure differentials using 4-point measurements. Its flexibility has benefits: it can withstand impact better than a rigid sensor, and it can be easily configured to match the surface it is placed on, such as a boat or other hydrodynamic vehicle. Its flexibility also gives it higher sensitivity to small pressures, providing a significant piezoresistive response at lower strains.

In order to achieve higher sensitivity, a lower elastic modulus was desired for the sensor. For this reason, CB-doped PDMS foam is being explored. Its feasibility depends on its ability to detect small strains and provide significant piezoresistive response. The ability to waterproof the sensor is also crucial; any coating must not diminish the sensitivity of the sensor. (9) In order to remove the necessity for a waterproof coating completely, a closed-cell foam is being explored.

Background

Silicone rubbers are polymeric elastomers, which exhibit non-linear elastic behavior different than linear elastic materials. For this reason, linear elastic models do not capture the behavior of elastomeric materials. The mechanical behavior of the sensor will therefore be non-linear elastomeric, exhibiting recovery of shape even after being subjected high stresses and large strains. The mechanical behavior of silicone, however, is dependent upon its processing conditions before testing and rate of strain during testing.

CB-PDMS, both the foam and its solid counterpart, are piezoresistive, meaning that under some change in strain, there will be a change in resistance in the material. This

piezoresistive nature is theorized to occur by the connecting network of CB particles in the PDMS matrix. Once a certain threshold of CB dopant is reached, enough conductive pathways will form to allow conduction through the material. Under strain, these conductive pathways are disrupted, but reform after some time. It has been theorized that the piezoresistive nature of this material can be attributed to the collapse of conductive pathways upon the straining of the material. (10) If this is the case, the resistance of the material would increase upon straining, as the collapse of these pathways would hinder conduction.

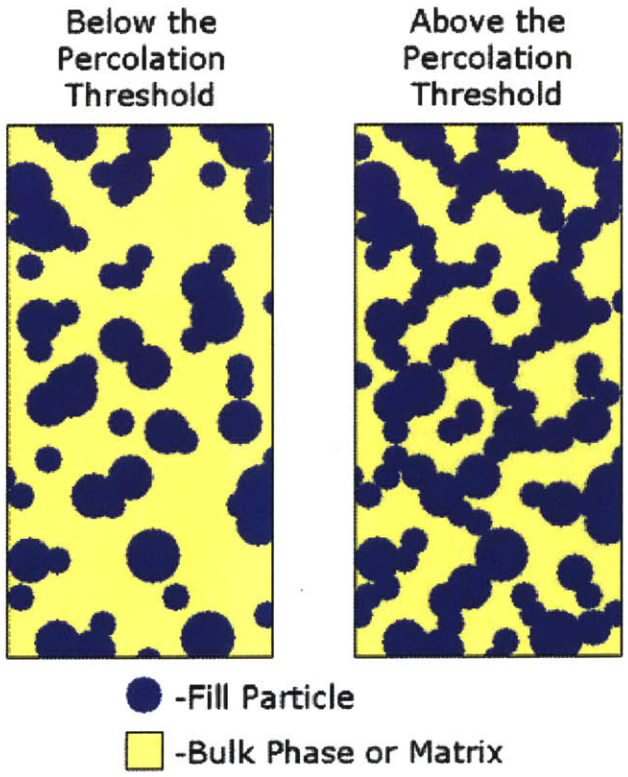

Figure 3. Representation of the percolation threshold, the concentration at which particles in a matrix form connected networks. Image from TDA (11).

This so-called percolation threshold of a matrix and filler particles – in this case, a silicone matrix with CB filler – occurs when the filler particles are at a high enough concentration to form interconnected networks of touching particles within the matrix. In order to approximate the volume fraction of CB needed to reach the percolation threshold, each cell wall was modelled simplistically as a 3D slab. The volume fraction of filler falls between a range of 0.3-0.4 using a slab as a model (12), and so the value 0.30 was chosen to approximate the percolation threshold for one cell wall, and by extension, the foam. This was done to verify the volume fraction range of CB to be used to dope the silicone foam. This calculation can be seen in Appendix A.

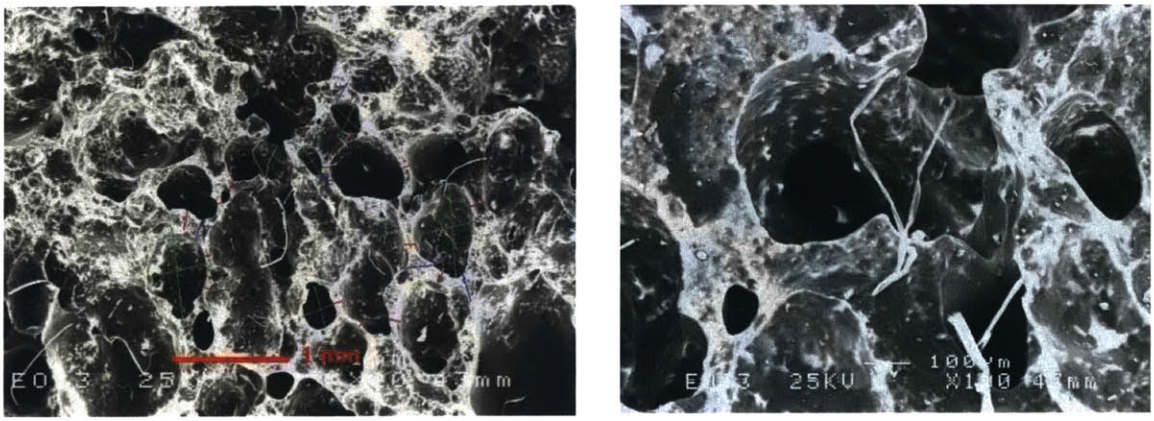

Figure 4. Images of 4 wt% CB-PDMS foam, taken at 20x magnification and 100x magnification, respectively. These images were used to calculate the cell geometry to predict the percolation threshold using ImageJ software.

The approximate percolation threshold mass CB per volume foam was calculated to be 0.64 g for a 2.5 cm long cube using the dimensions of a cell wall measured using an SEM. The cube samples were approximately 10 g in mass, giving a weight percent of 6.4%. This model is an over-estimation – the cell walls are thinner near the middle and thicker near the joining edges, and as such will not behave exactly like a slab would. In addition, previous work with this material has shown that weight percent ratios near 3-5 wt% had been optimal. For these reasons, ratios from 4 to 5.5 wt%, in 0.5 wt% increments, were studied.

Materials and Methods

Waterproofing the open-cell PDMS foam proved to be a challenge. (8) A number of materials and procedures were employed to ensure that water would not disrupt the mechanical behavior of the foam, such as Saran wrap and a pure, solid PDMS coating, but Saran wrap was not a structurally sound solution and solid PDMS became the dominant mechanical material in the device, limiting the foam's ability to sense pressure differences. In order to combat this problem, a closed-cell foam was employed so that water could not make its way into the foam material. A commercially available closed-cell foam was procured from Smooth-On.

Smooth-On product *Soama Foama 15* was used to make the sensors because of its relative chemical similarity to the PDMS foam, its closed-cell structure, and its quick production time. The PDMS foam required 20 minutes to cure at 120 degrees and a water

bath for 24 hours at 80 C in order to leech out sugar, which was used as a sacrificial scaffold. *Soama Foama 15* (herein referred to as SF15) is a low-density closed-cell foam with a cure time of one hour in ambient conditions, making production of SF15 sensors much more efficient than production of the previous PDMS foam sensors.

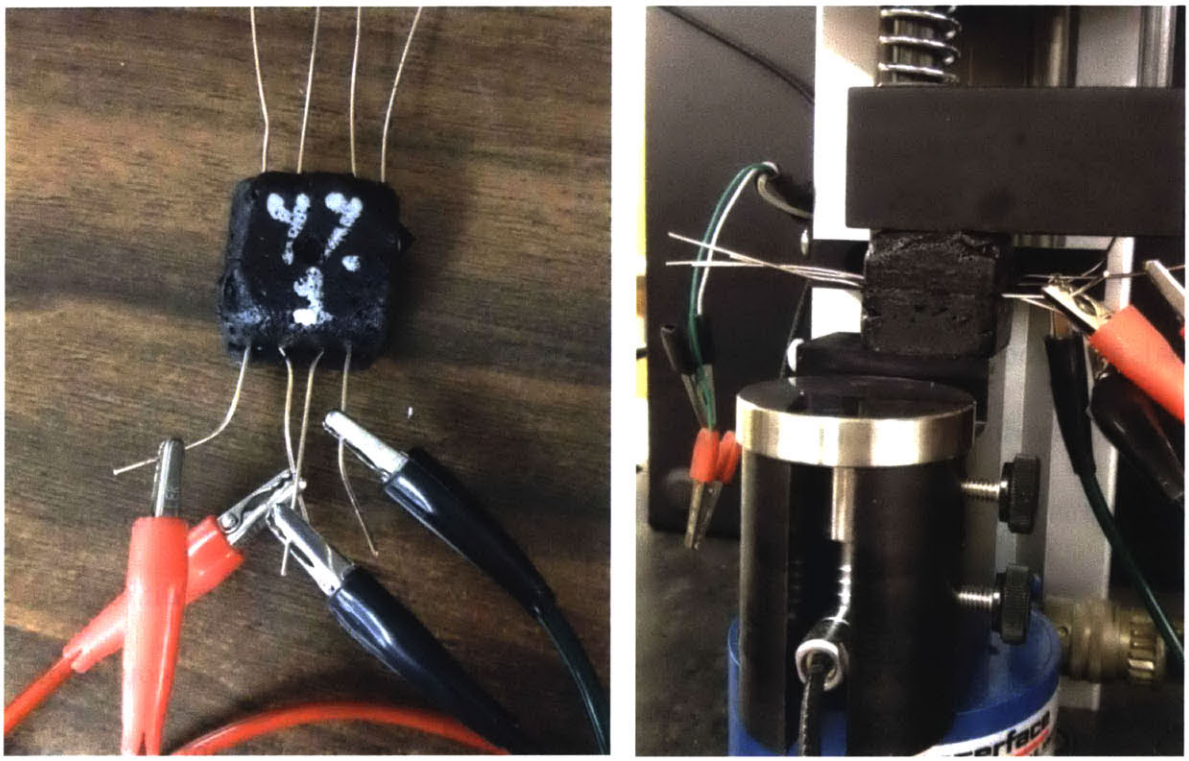

Figure 5. Wiring arrangement (left) and compression testing (right) using Keithley Sourcemeter and custom ADMET instrument.

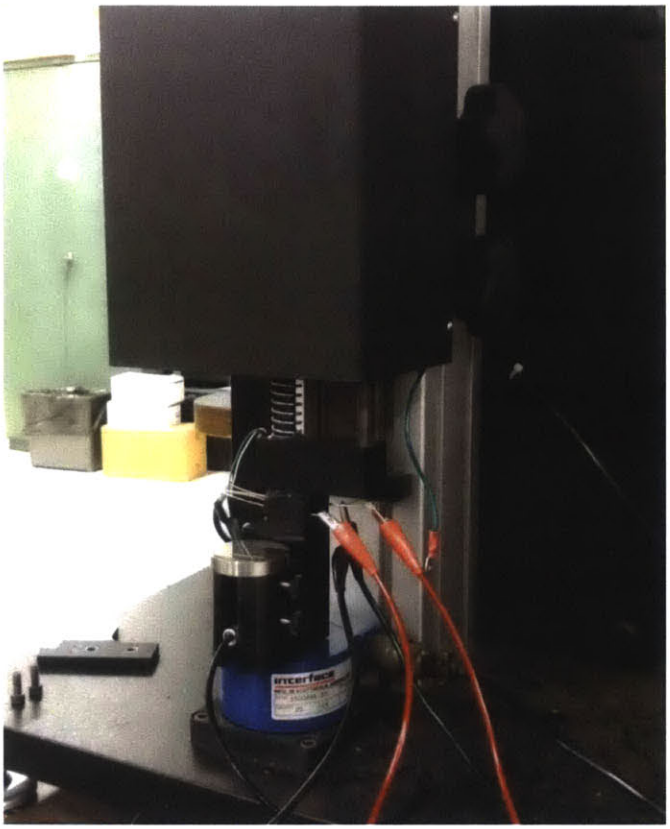

Figure 6. ADMET mechanical testing instrument used in experiments.

Pure SF15

SF15's production procedure was optimized by Smooth-On. Two parts, Part A and Part B, liquid components provided by Smooth-On, were used. Two parts A and one part B by weight were drawn out using a 3 mL syringe and released into a mixing cup. Both parts were then mixed well together by hand for approximately 10 seconds. The mixture was quickly poured into a mold before the material had become solid and no longer pourable, which occurred after approximately 2 minutes. The foam was then allowed to cure, expanding approximately 2-3 times its original volume when foamed fully.

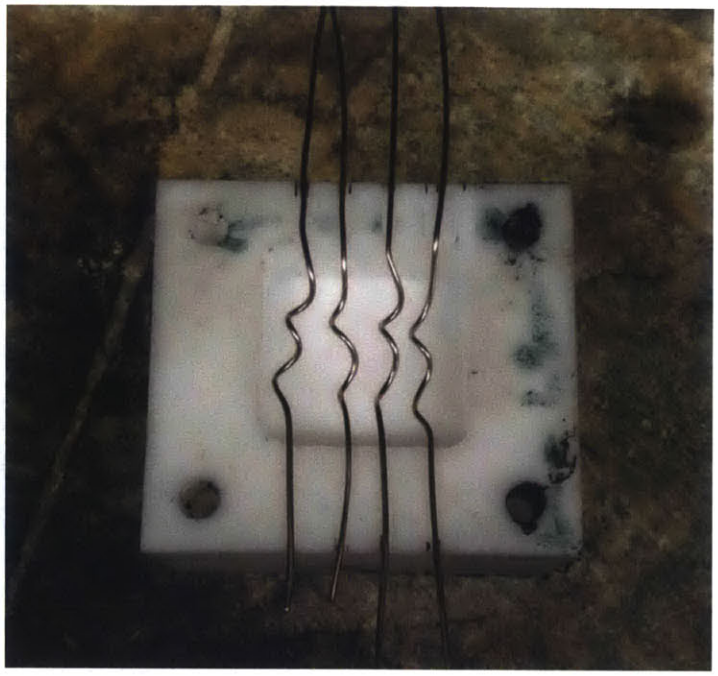

Figure 7. Mold used to shape foam. Foam poured under wires, then wires were placed on top of expanding foam. A top identical piece was placed on top and screwed down until tightened to ensure full molding around wires.

Carbon Black-doped SF15

Two parts A was measured out by weight and released into a mixing cup using a 3 mL syringe. Carbon Black (herein called CB) was measured out by weight under a fume hood and mixed in with Part A until uniform. Mechanical mixing provided good uniformity, but the heat from mixing at times caused early curing and solidification of the incomplete mixture. Samples were mixed by hand to avoid mechanical heat and early curing. One part B was added to the mixed CB-doped A. This was mixed by hand for approximately 10 seconds, and quickly poured into the mold. The foam was allowed to cure

for one hour, expanding to 3-4 times its original volume. Adding larger amounts CB would cause the foam to expand less, although still approximately in the range specified above. The exact expansion of each sample was not calculated.

In order to measure piezoresistive responses from the foam, wires were molded into the samples as well. As soon as the foam was poured into the mold, wires were placed on top. The top of the mold was placed on top of the wires and bottom half of the mold. Four wires were placed in the samples, allowing for four-point measurements of voltage to be recorded with reasonable accuracy, even with the presence of contact resistance.

Mechanical and Electrical Property Measurement

Mechanical properties of the foam were measured using a custom-built ADMET mechanical testing apparatus and the ADMET MTESTQuattro and NI LabVIEW software. The measurement profile was programmed using the MTESTQuattro software and implemented on the ADMET. Voltage was measured using a NI-DAQ board and a custom NI LabVIEW program. A number of different profiles were constructed and used, and are explained in the Results section.

The electrical response of the foam to mechanical pressures was recorded during mechanical tests. A current was sent through the foam so as to record a significant voltage difference measurement upon adding pressure to the sample. A Keithley 2602 Sourcemeter was used to apply a current to the sample and a NI-DAQ board to measure the voltage response in LabVIEW. A current of 0.1 mA was applied in all cases except the 5.5 wt%

samples, which were measured with 0.5 mA due to the magnitude of the recorded voltage being too low to read precisely.

Mechanical testing was performed on each sample, recording the voltage measured in the sample as a function of time in addition to force and position.

Results

Mechanical Properties

The mechanical behavior of the samples at high strain shows the beginning of densification around 30% strain in each sample, in the range of 20-30 kPa stress. While there is no true linear-elastic regime, an elastic modulus can be calculated for the regime ranging from approximately 0.02 to 0.3 due to its linearity. One expects that the composite materials will have a higher elastic modulus than the undoped silicone foam due to the Rule of Mixtures; however, due to the small difference in weight percent dopant between samples, this difference should be small. This is evidenced from the data as well.

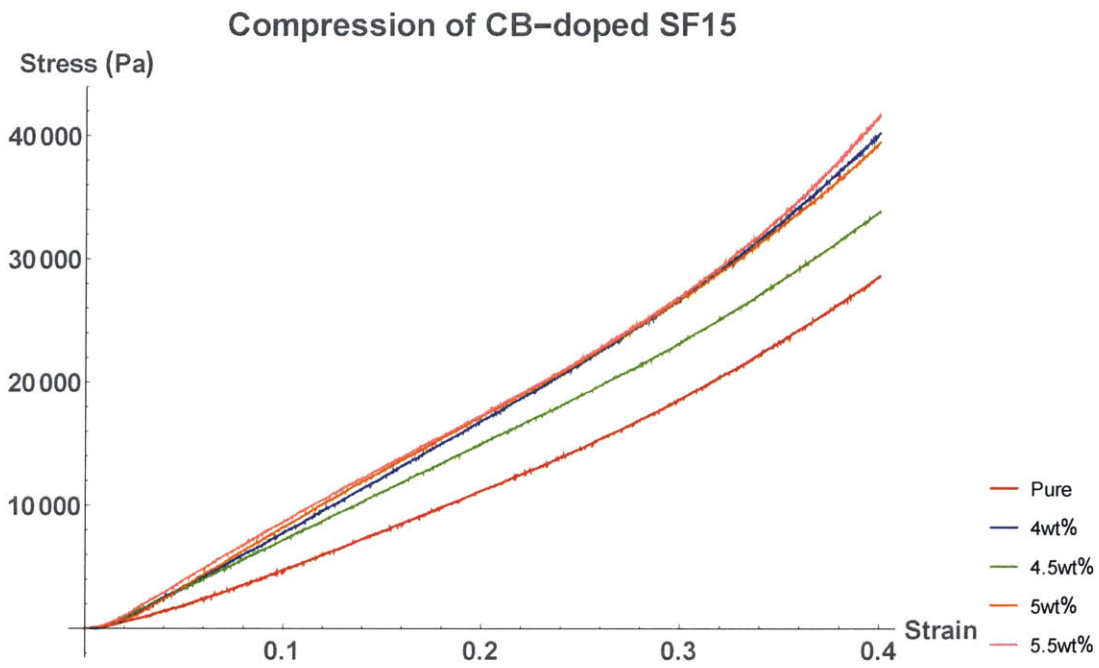

Figure 8. Compression test results for all tested samples. Non-linear elastic behavior is observed, in accordance with expectations of a non-linear elastic material such as PDMS. Most samples exhibit similar magnitude of behavior, and any discrepancy may be due to unfilled molding or air pockets in sample.

Piezoresistive Properties

The doped foam samples were tested mechanically while recording voltage response from the material. A test procedure was developed to record changes in voltage from a strain pattern in order to determine whether the sensor could respond quickly enough to the strain pattern to detect the waves. Two strain patterns were tested: a varying frequency sinusoidal test (amplitude: 8% strain), and a constant strain rate (5 mm/min, 20% strain) ramp. Voltage was measured as a function of time, as was force and position of the platen.

4 wt% ratio

Ramp

This simple ramp was performed at a strain rate of 5 mm/min. The sample was compressed to 20% strain and then returned to 0% strain. Hysteretic behavior is observed: the amount of force required to strain the sample is larger when compressing than when decompressing. An elastic modulus, though not a linear model, can be calculated for this range of strain in order to predict mechanical behavior.

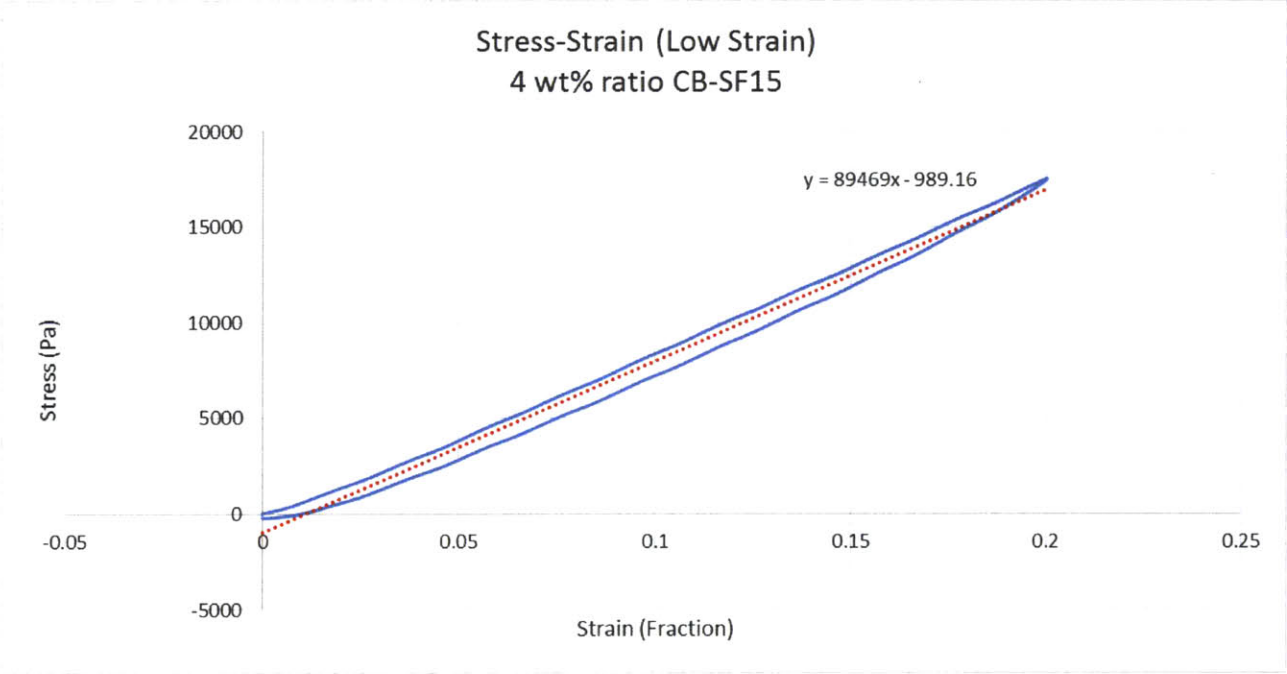

Figure 9. Compression to 5 mm, or 8%, and back down to equilibrium. Elastic modulus given by slope of fitted line.

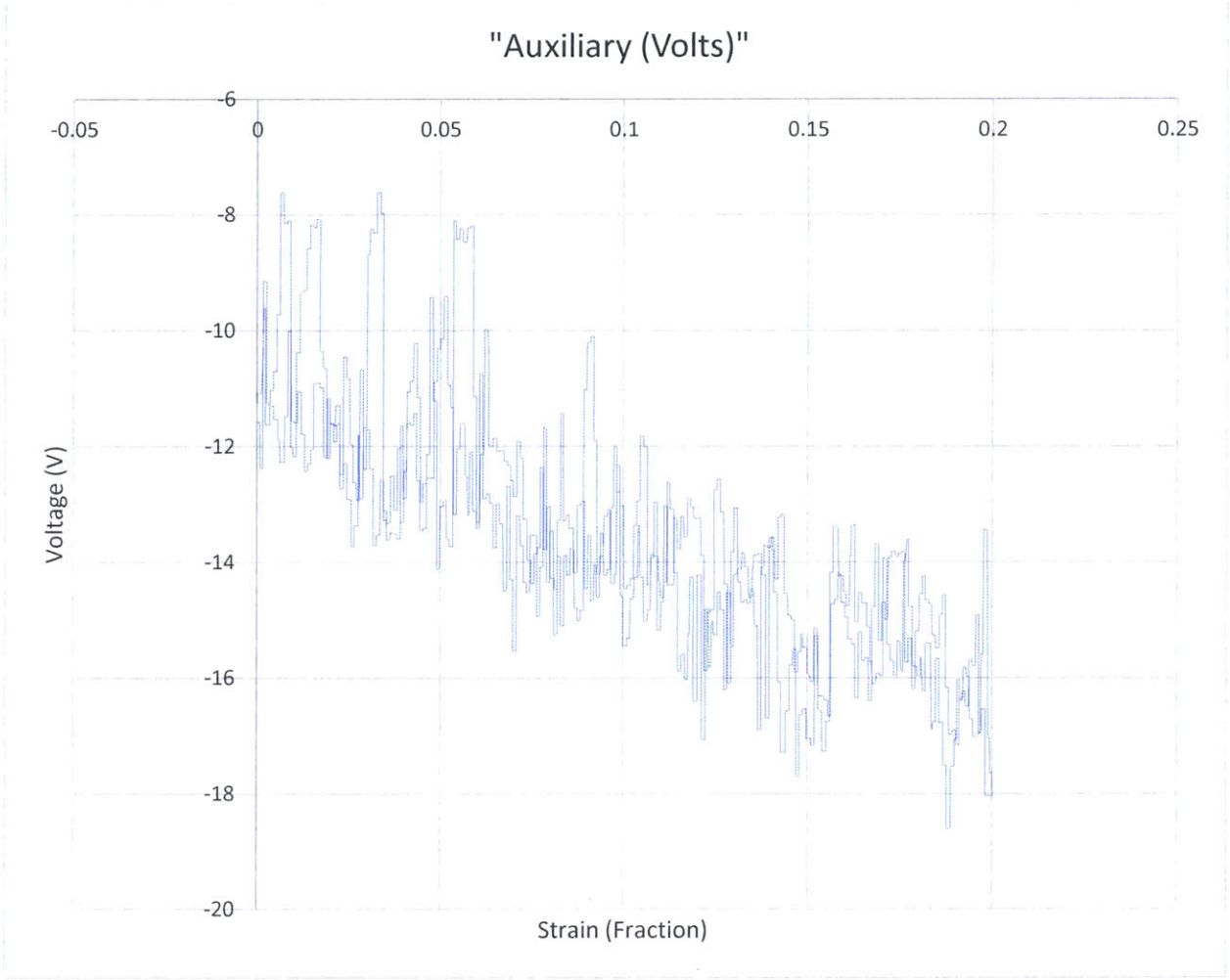

Figure 10. Voltage measured as a function of strain. Hysteretic behavior observed, although large amounts of noise are present.

Hysteretic behavior is observed in voltage response as well. Even with the large amount of noise present, the voltage observed in compression follows a similar pattern to that observed during tension, and each regime behaves similarly. Higher compression results in a higher recorded voltage.

Sinusoidal Frequency Sweep

Hysteretic behavior is clearly observed in the stress-strain plot (Figure 11) below. This test included two regimes, started from a pre-loaded condition: 10 cycles of 0.5 Hz frequency sinusoid, 10 cycles of 1 Hz frequency sinusoid, and the same for frequencies of 2 Hz and 4 Hz. The frequency shows little influence on the hysteretic behavior; the material behaves similarly mechanically for these frequencies.

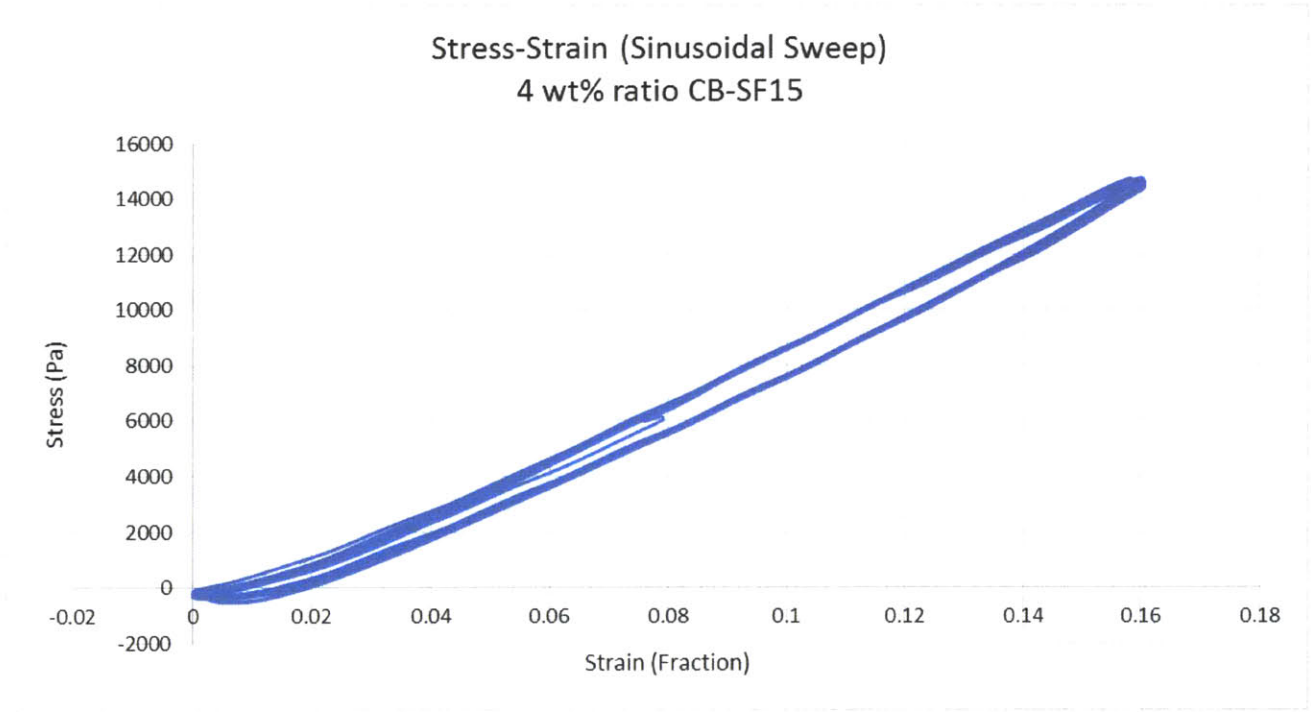

Figure 11. Hysteretic behavior is observed for each frequency.

At 0.5 Hz frequency, the material senses with some clarity the changes in stress. However, at 1 Hz, the ability to sense changes in strain becomes much more difficult, although possibly due to noise levels. At the highest tested frequencies, 2 Hz and 4 Hz, 4 wt% CB-PDMS cannot detect accurately the changes in applied pressure.

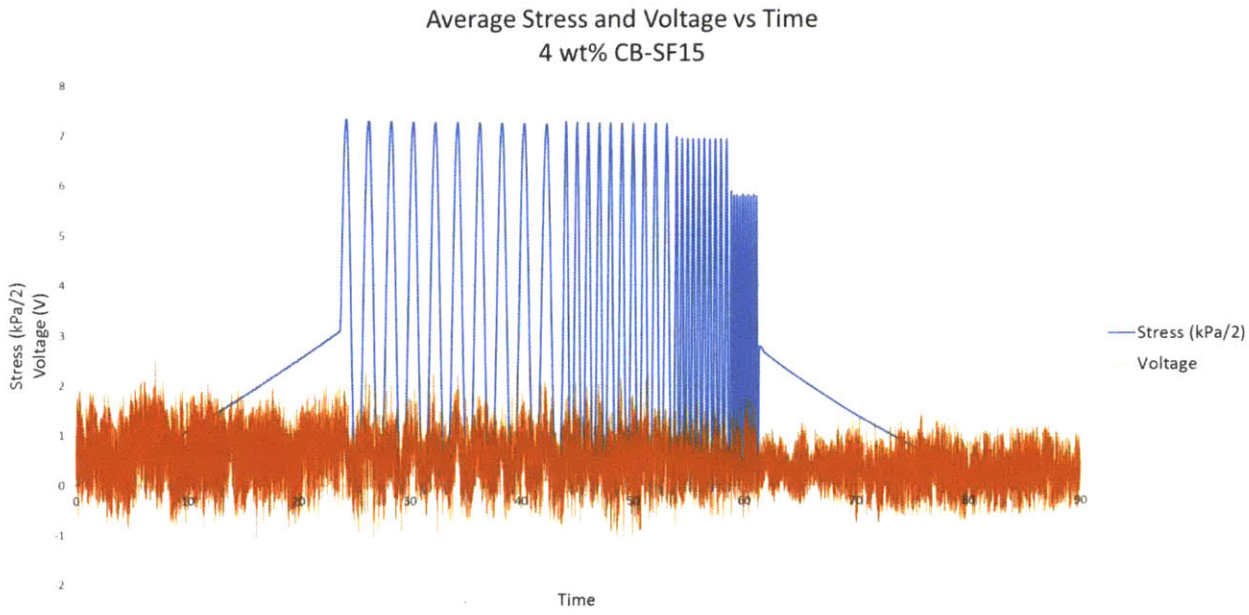

Figure 12. Normalized stress and voltage as a function of time. Responses are difficult to see at such a large scale.

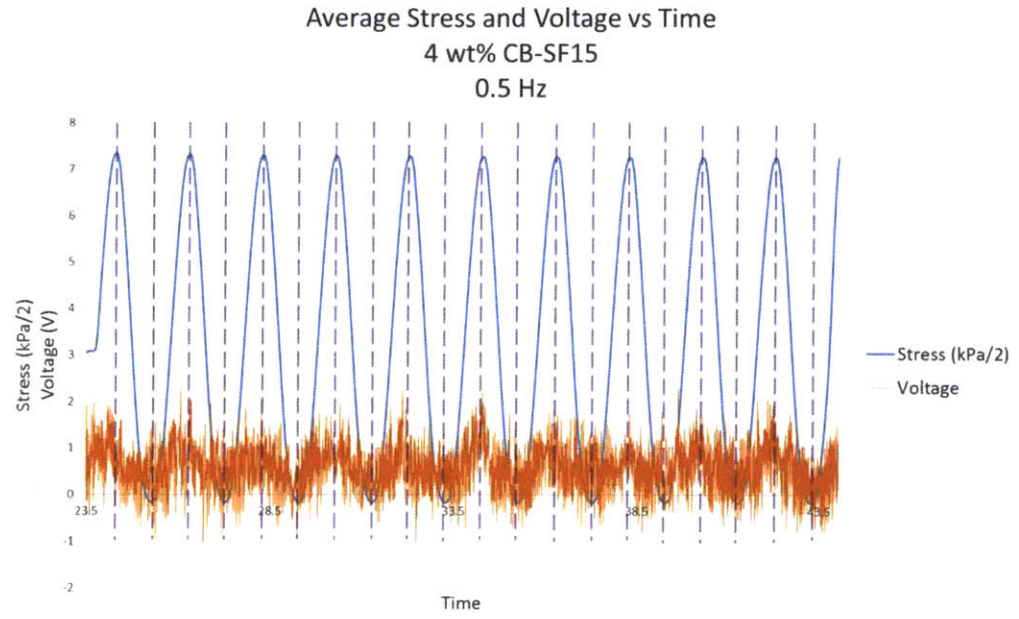
Average Stress and Voltage vs Time
4 wt% CB-SF15
0.5 Hz
Stress (kPa/2)
Voltage (V)
Time
Stress (kPa/2)
Voltage

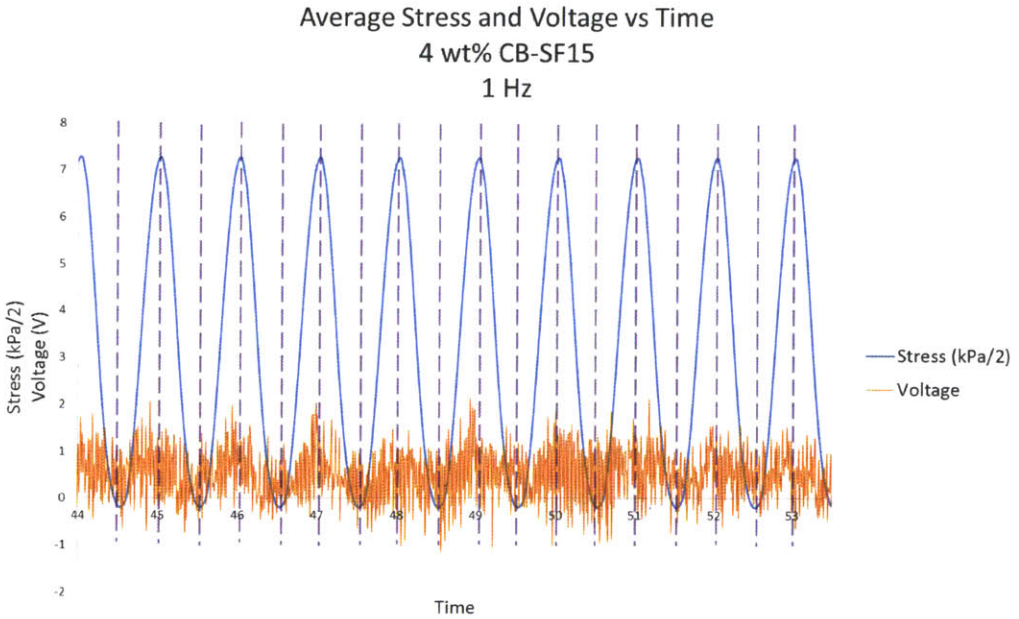
Average Stress and Voltage vs Time
4 wt% CB-SF15
1 Hz
Stress (kPa/2)
Voltage (V)
Time
Stress (kPa/2)
Voltage

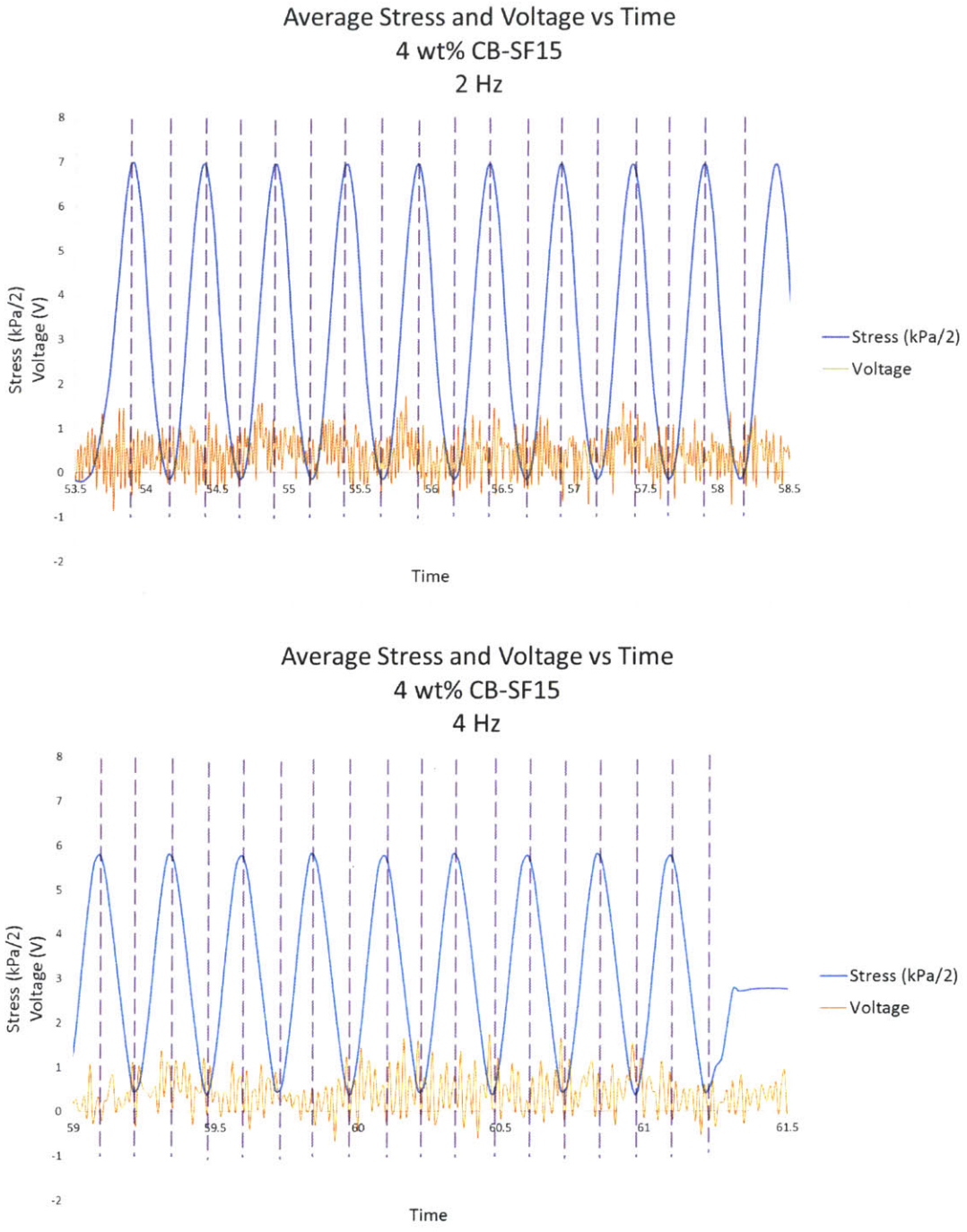

Figure 13. Stress and Voltage, averaged over all tested samples, as a function of time. The 4 wt% ratio CB-PDMS is able to sense 0.5 Hz waves, but fails to sense accurately the other frequencies.

4.5 wt% ratio

Ramp

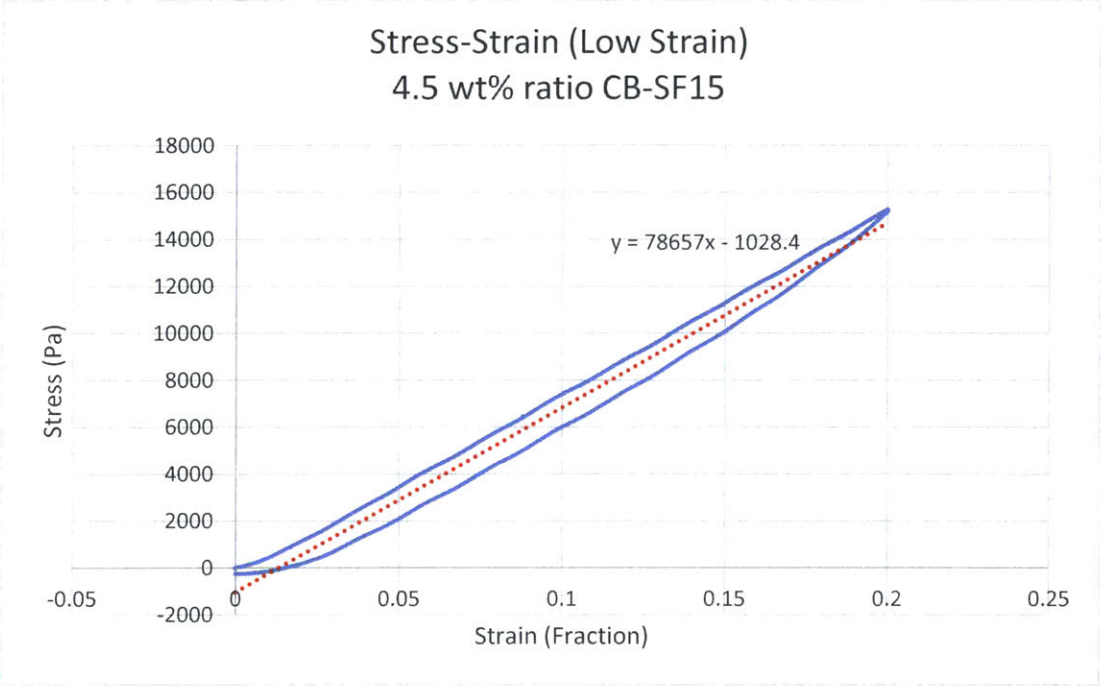

Figure 14. Compression to 5 mm, or 8%, and back down to equilibrium. Elastic modulus given by slope of fitted line.

The same experiments were performed on a 4.5 wt% sample of CB-PDMS. Again, mechanical hysteretic behavior is observed and an elastic modulus calculated. A hysteretic trend is also observed in the voltage response.

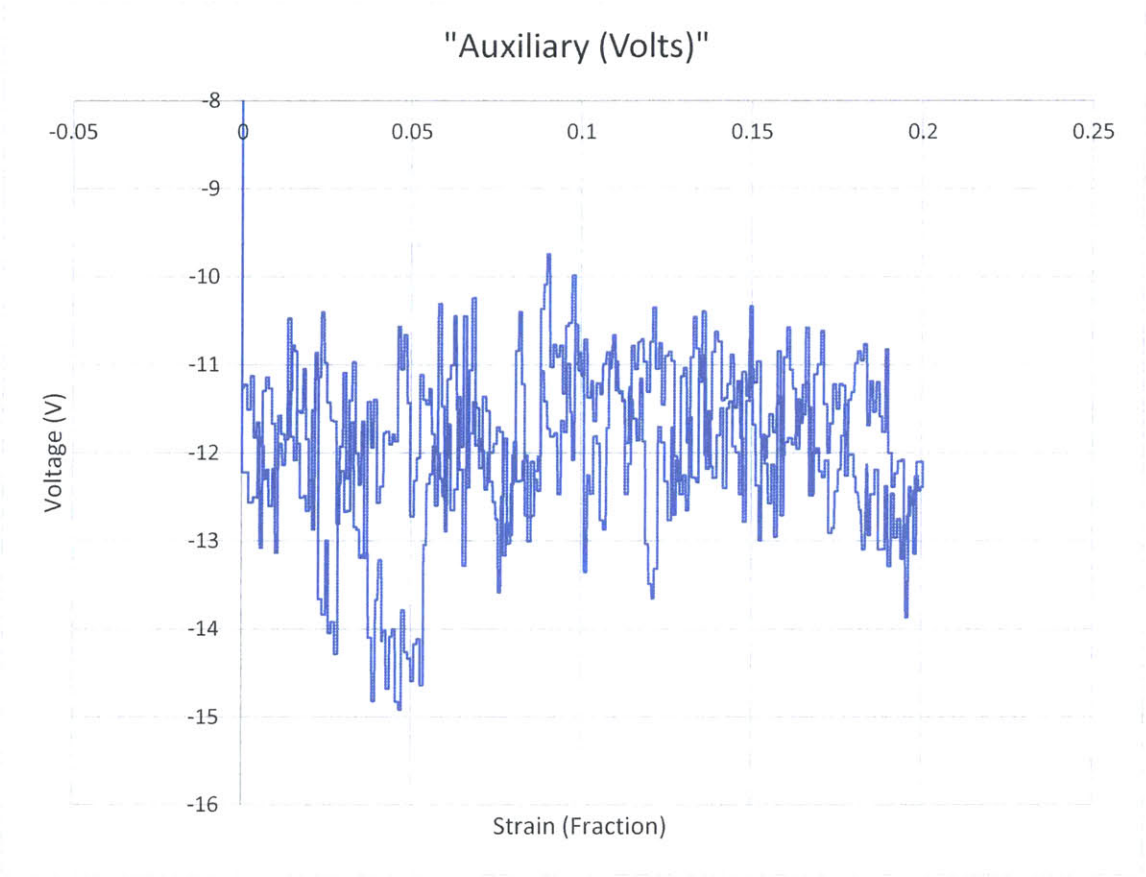

Figure 15. Voltage measured as a function of strain. Hysteretic behavior observed, although large amounts of noise are present.

Sinusoidal Frequency Sweep

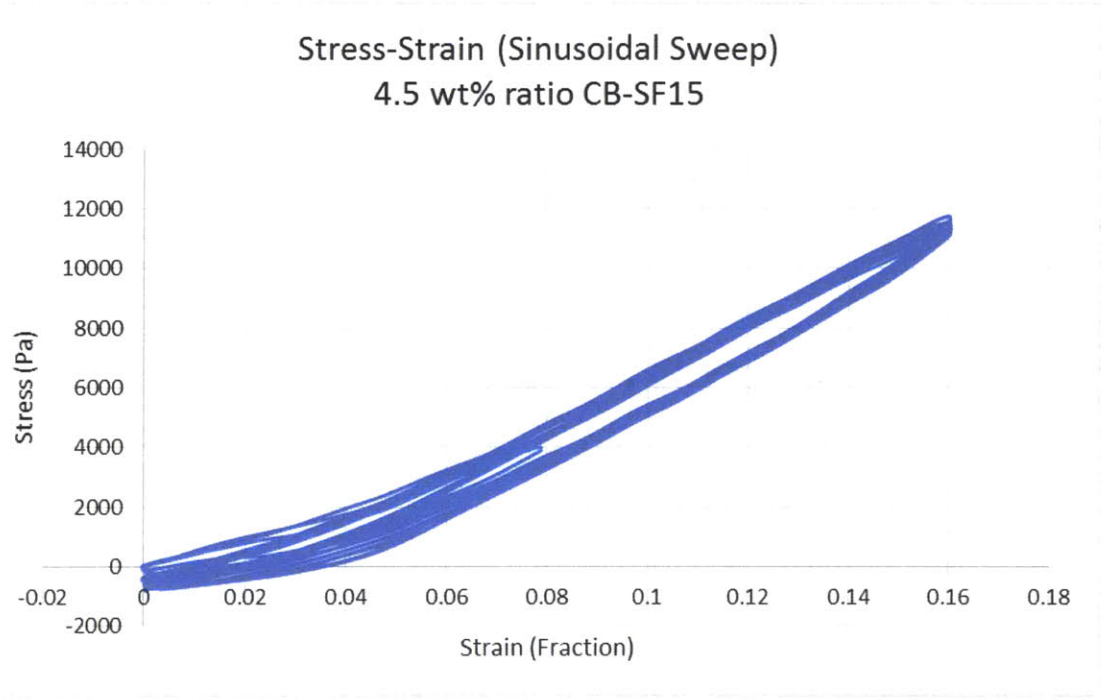

Figure 16. Hysteretic behavior is observed for each frequency.

For the 4.5 wt% material, sensing is difficult at even the lowest frequency. As frequency was increased, the material's sensing ability dropped.

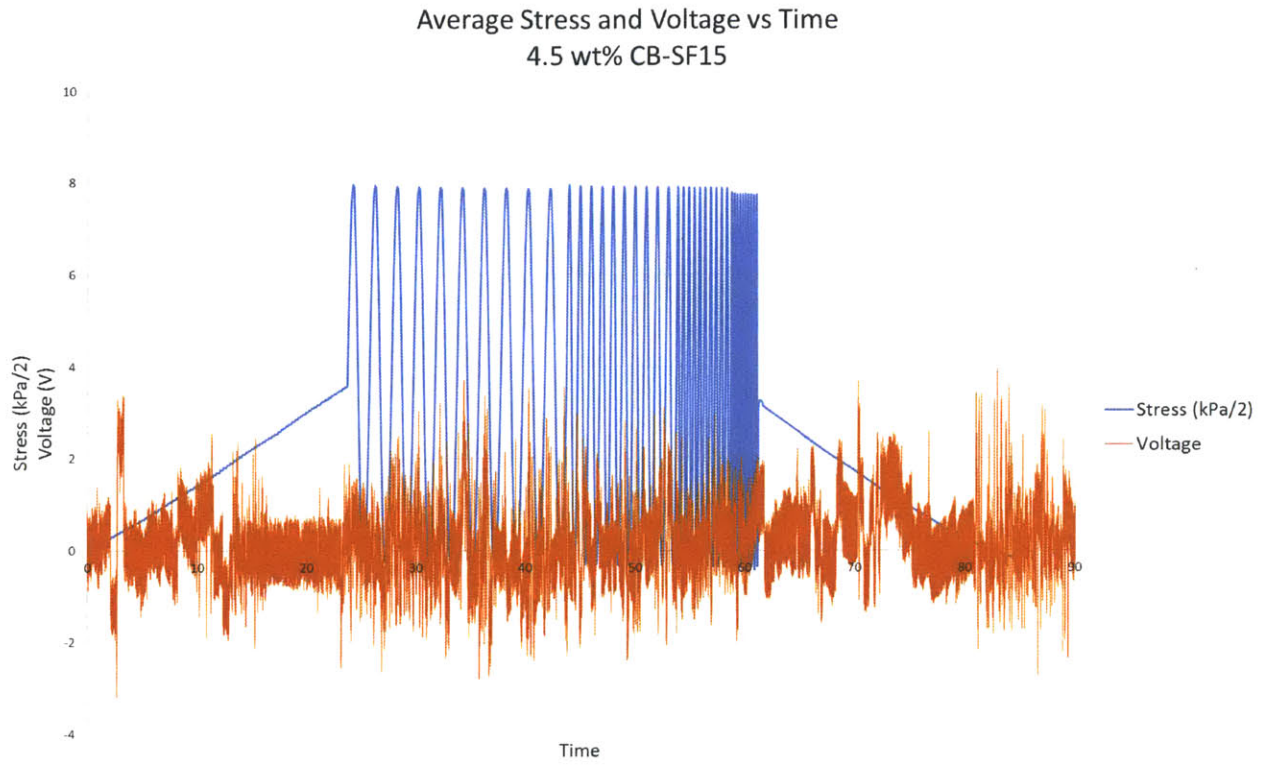

Figure 17. Full test procedure results. Sensitivity is difficult to see at this range.

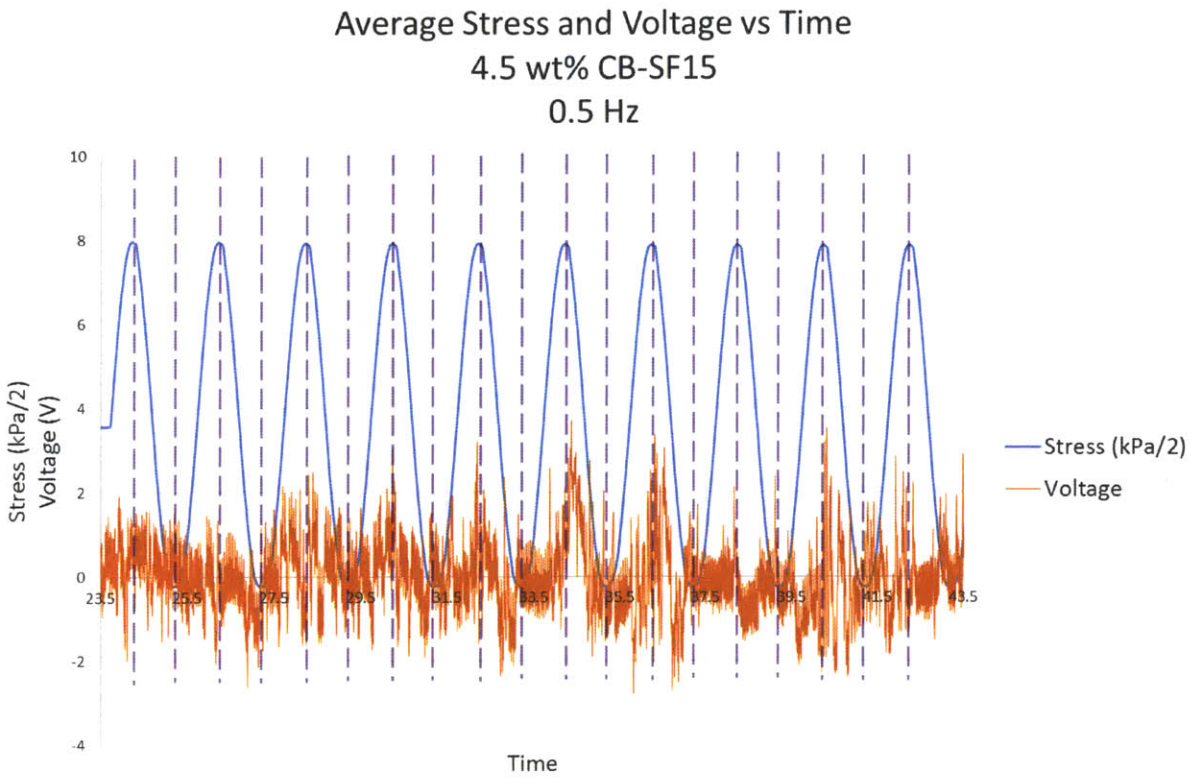
Average Stress and Voltage vs Time
4.5 wt% CB-SF15
0.5 Hz
Stress (kPa/2)
Voltage (V)
Time
Stress (kPa/2)
Voltage

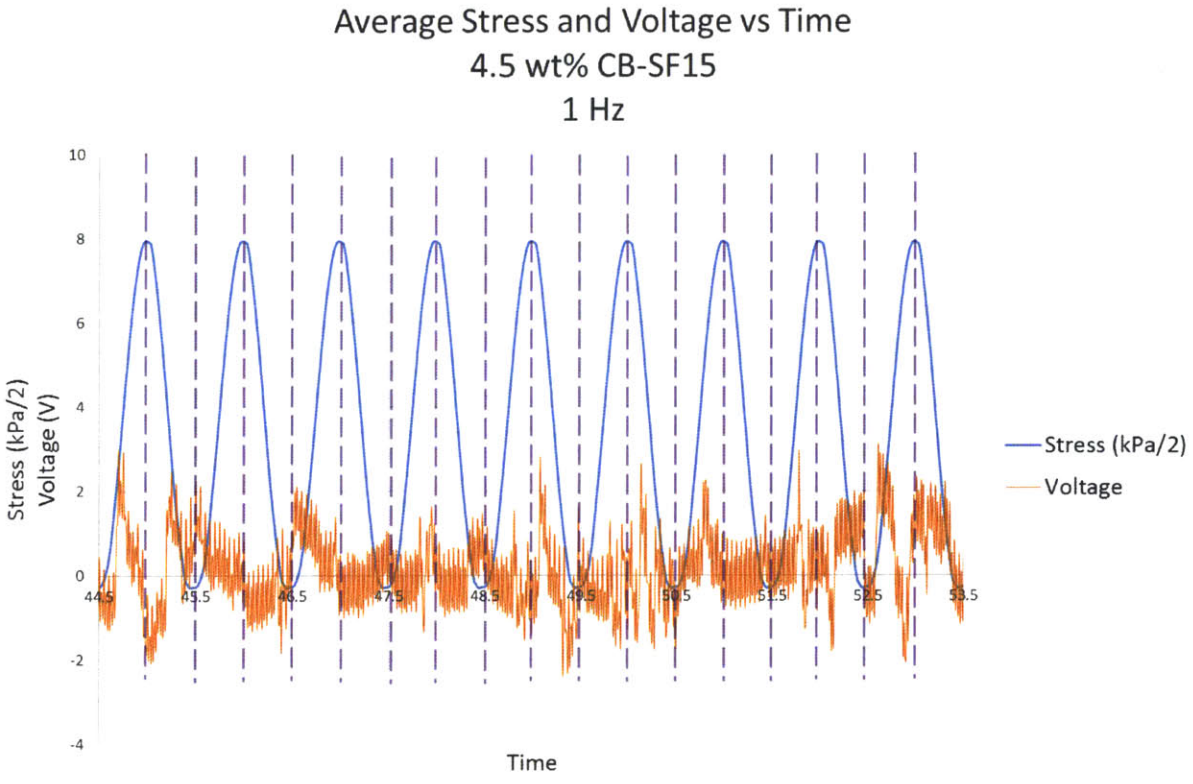
Average Stress and Voltage vs Time
4.5 wt% CB-SF15
1 Hz
Stress (kPa/2)
Voltage (V)
Time
Stress (kPa/2)
Voltage

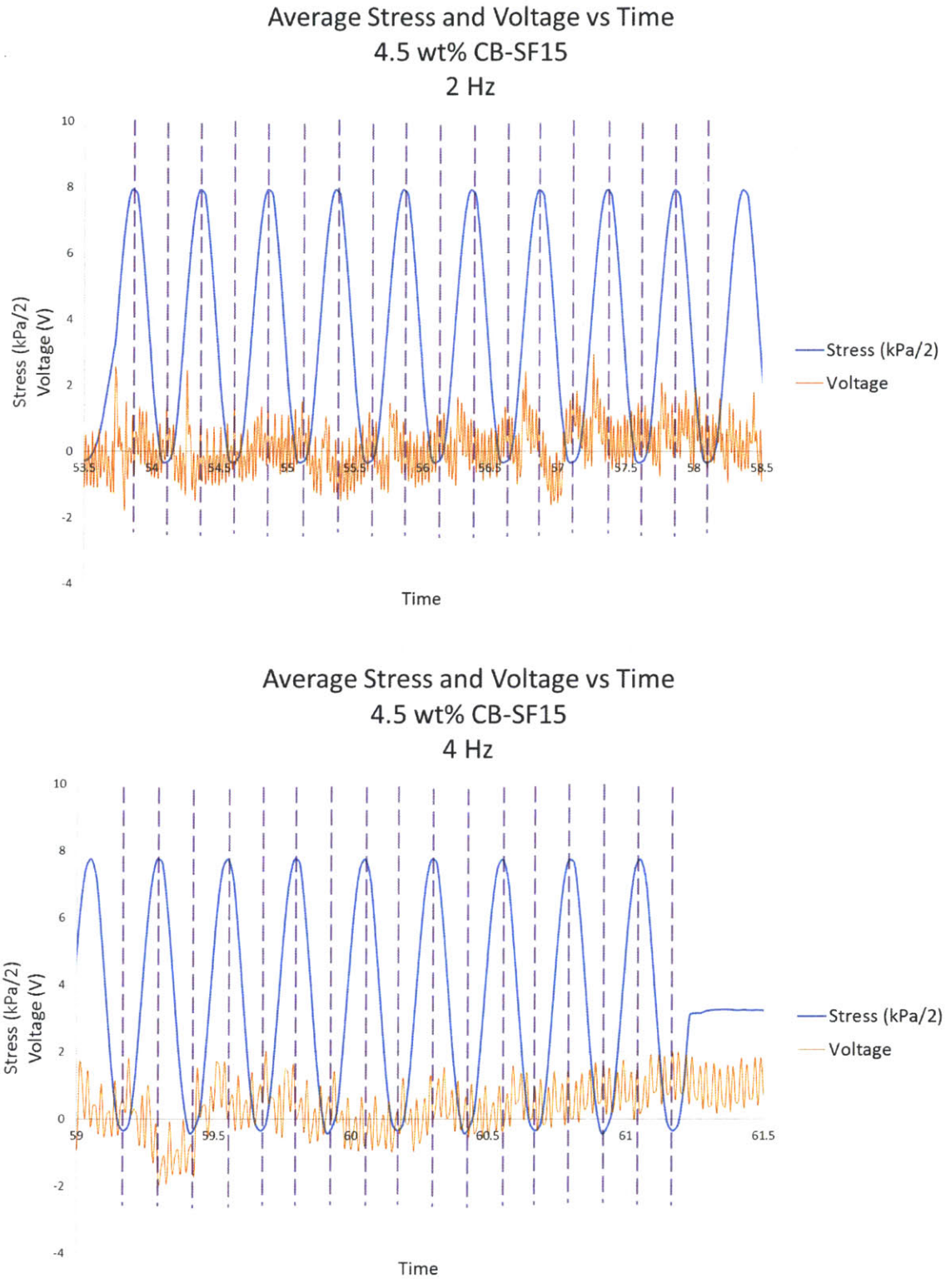

Figure 18. Sensitivity is very low for the 4.5 wt% sample, which barely senses even 0.5 Hz waves.

5 wt% ratio

Ramp

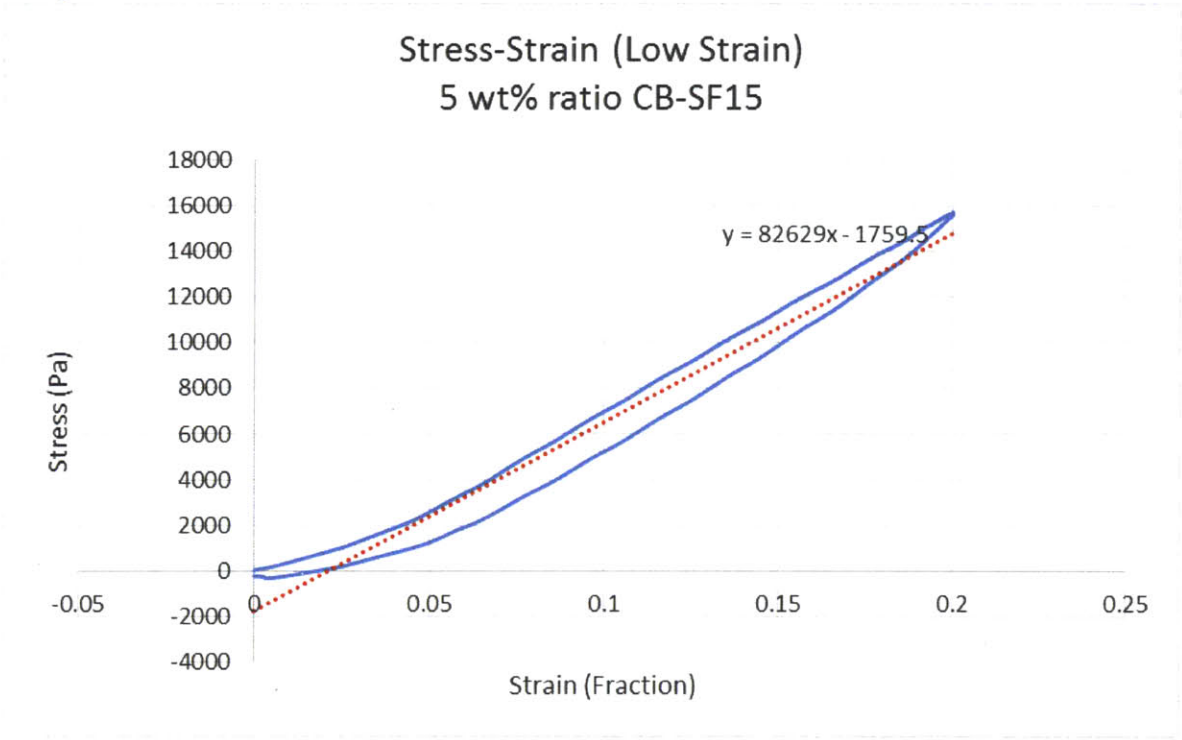

Figure 19. Compression to 5 mm, or 8%, and back down to equilibrium. Elastic modulus given by slope of fitted line.

Similarly to previous experiments, hysteretic behavior was observed in both the mechanical and electrical measurements. An elastic modulus was calculated.

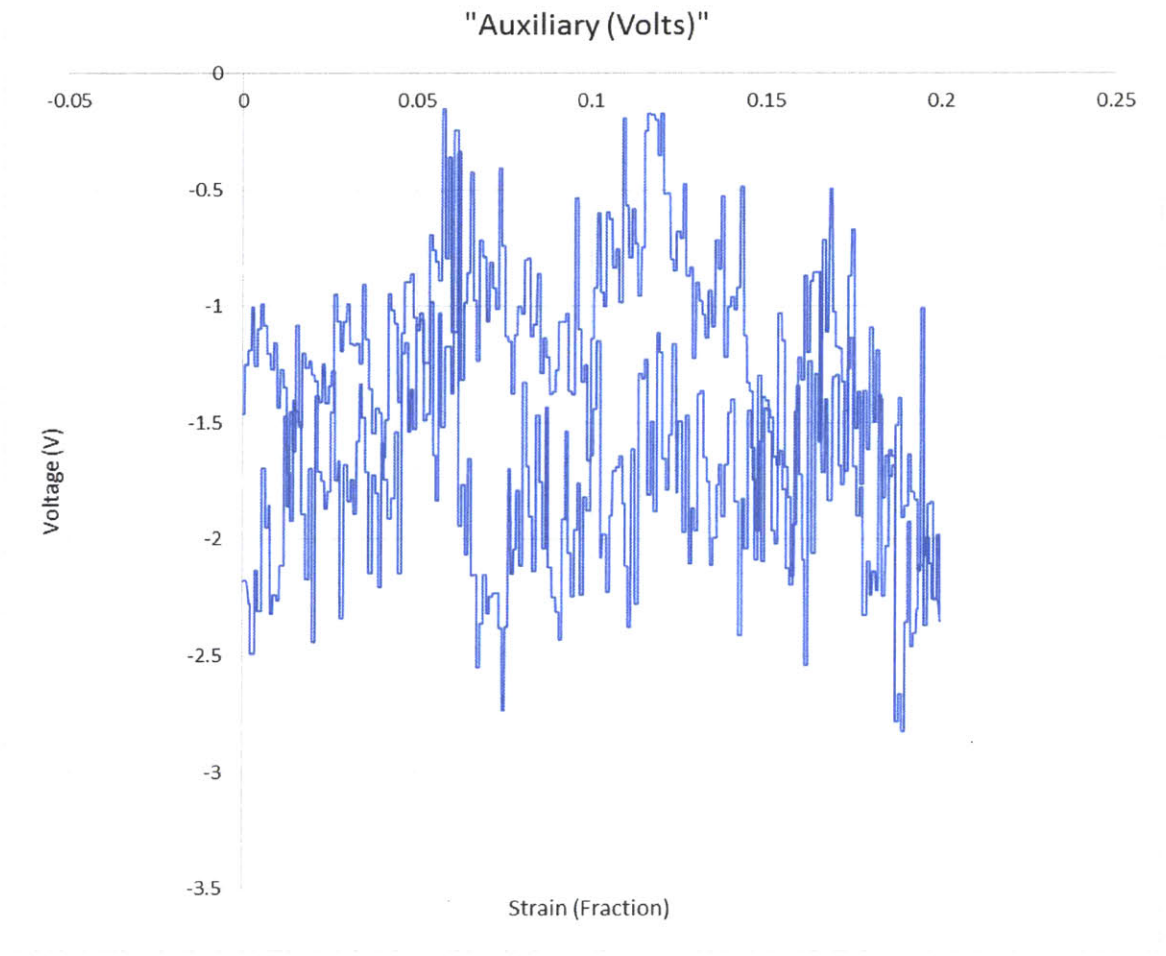

Figure 20. Voltage measured as a function of strain. Hysteretic behavior observed, although large amounts of noise are present.

Sinusoidal Frequency Sweep

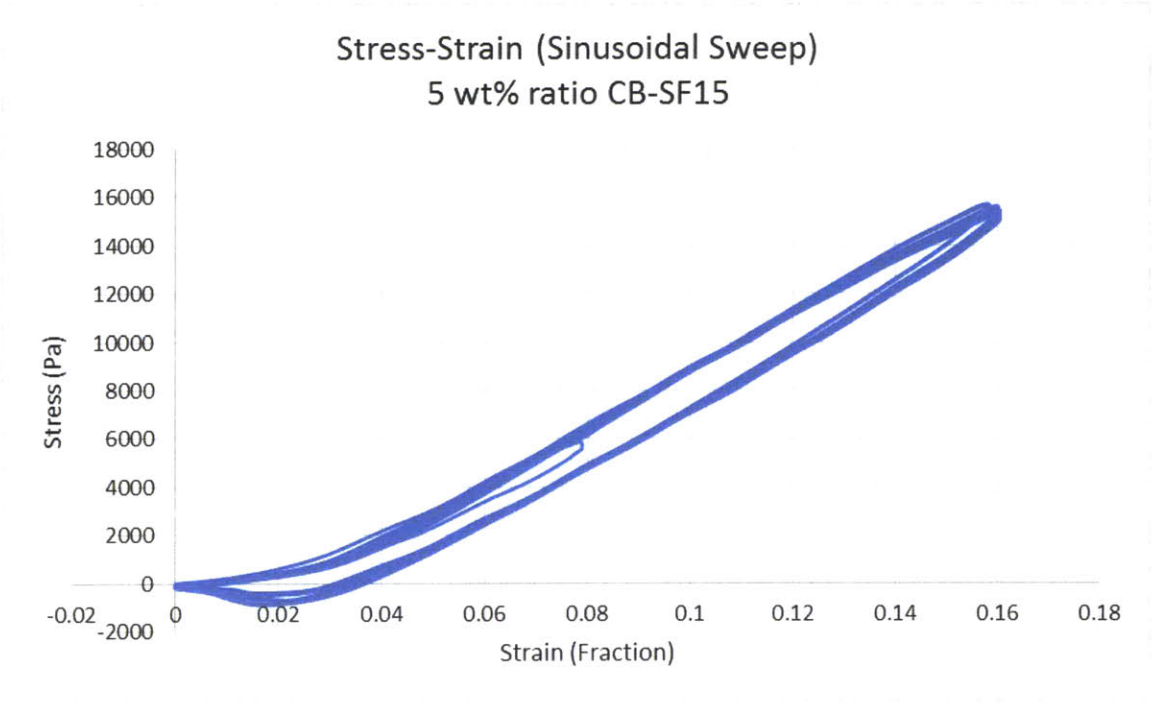

Figure 21. Mechanical behavior is similar across all tested frequencies.

The 5 wt% material was capable of sensing 0.5 Hz stimuli, but higher frequency measurements were difficult.

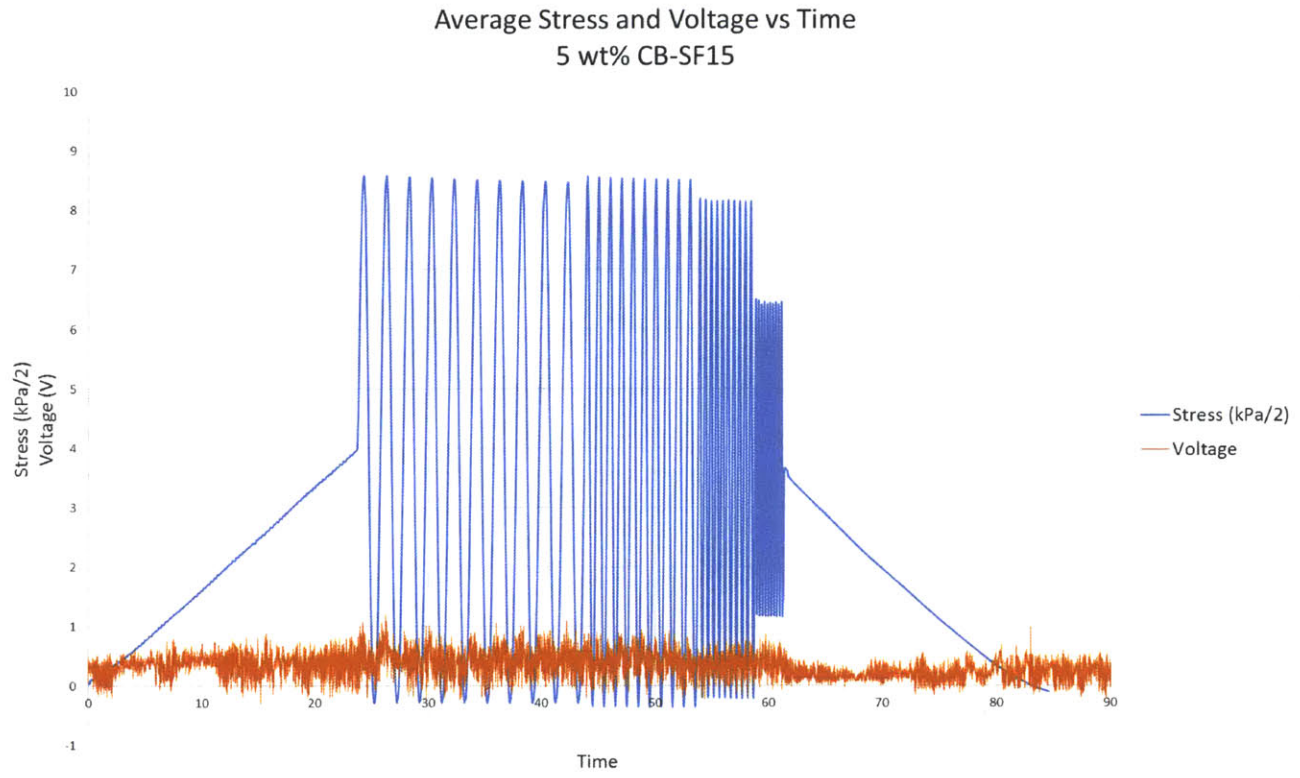

Figure 22. There is some sensitivity to 0.5 Hz waves in the 5 wt% samples, but sensitivity is lost with higher frequency. This is the entire test procedure result for the 5 wt% samples.

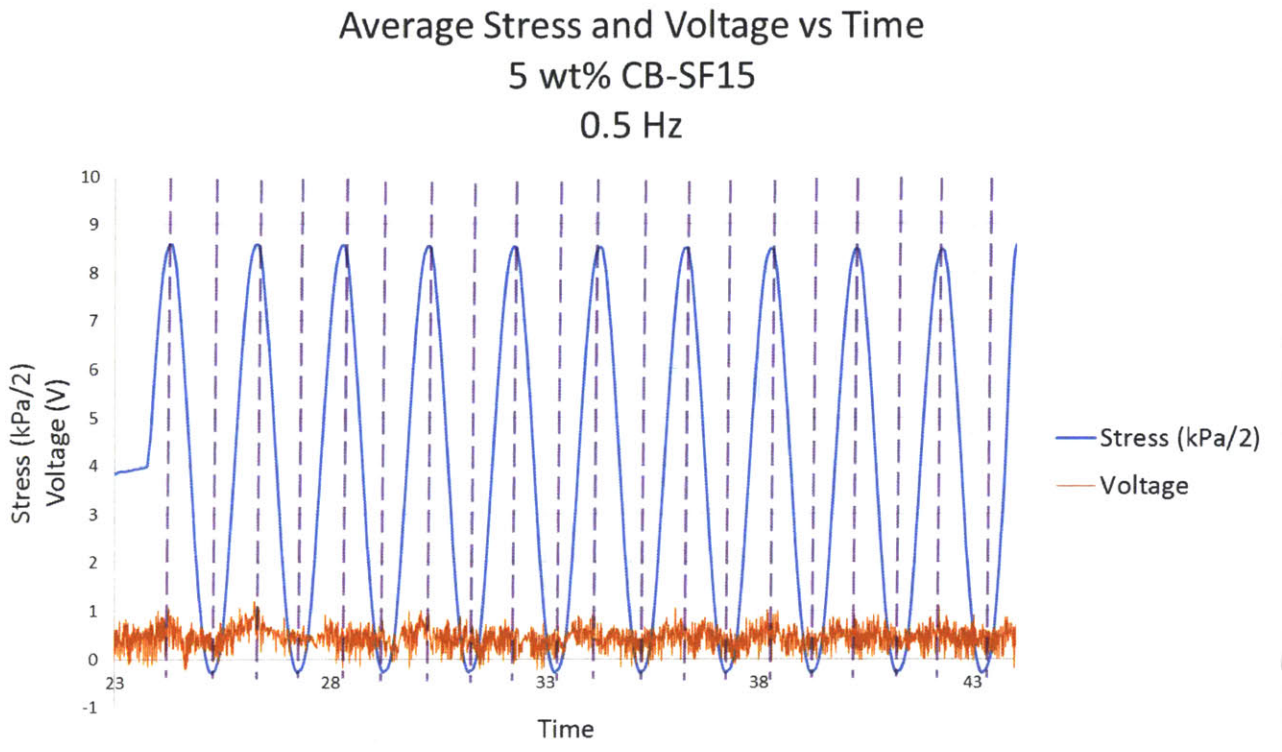
Average Stress and Voltage vs Time
5 wt% CB-SF15
0.5 Hz
Stress (kPa/2)
Voltage (V)
Time
Stress (kPa/2)
Voltage

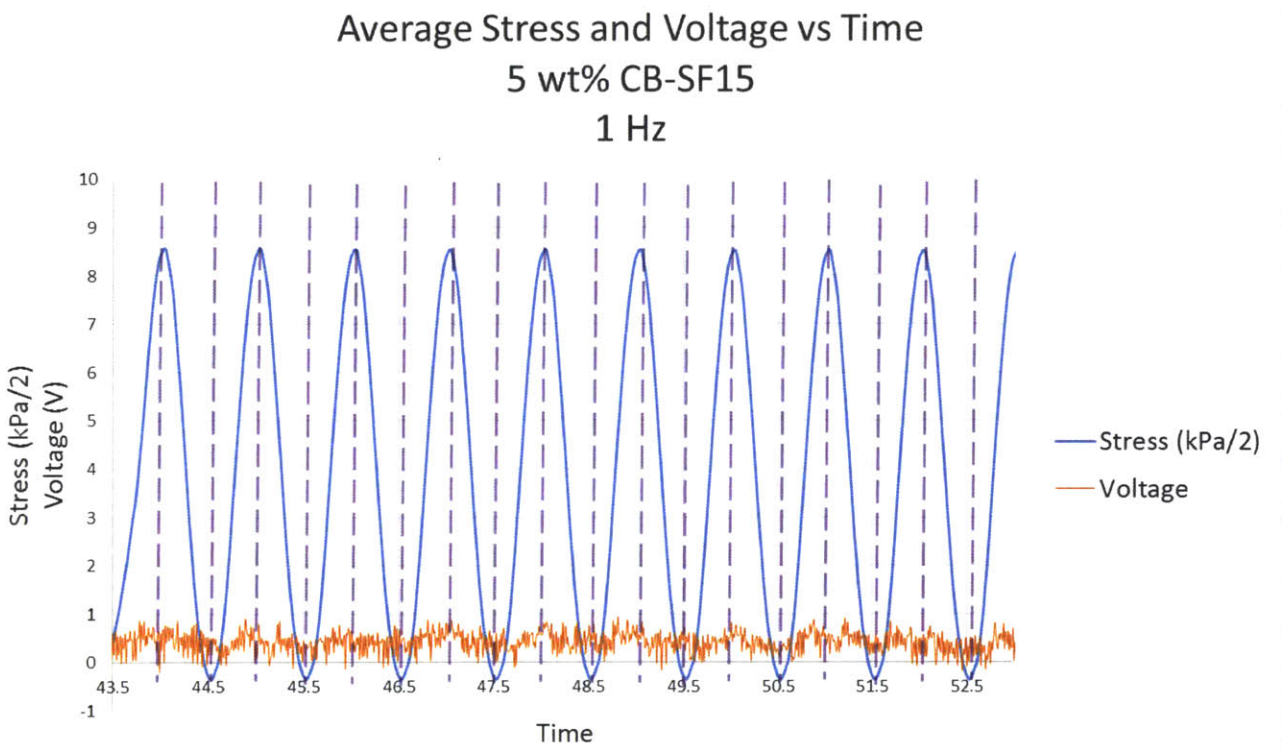
Average Stress and Voltage vs Time
5 wt% CB-SF15
1 Hz
Stress (kPa/2)
Voltage (V)
Time
Stress (kPa/2)
Voltage

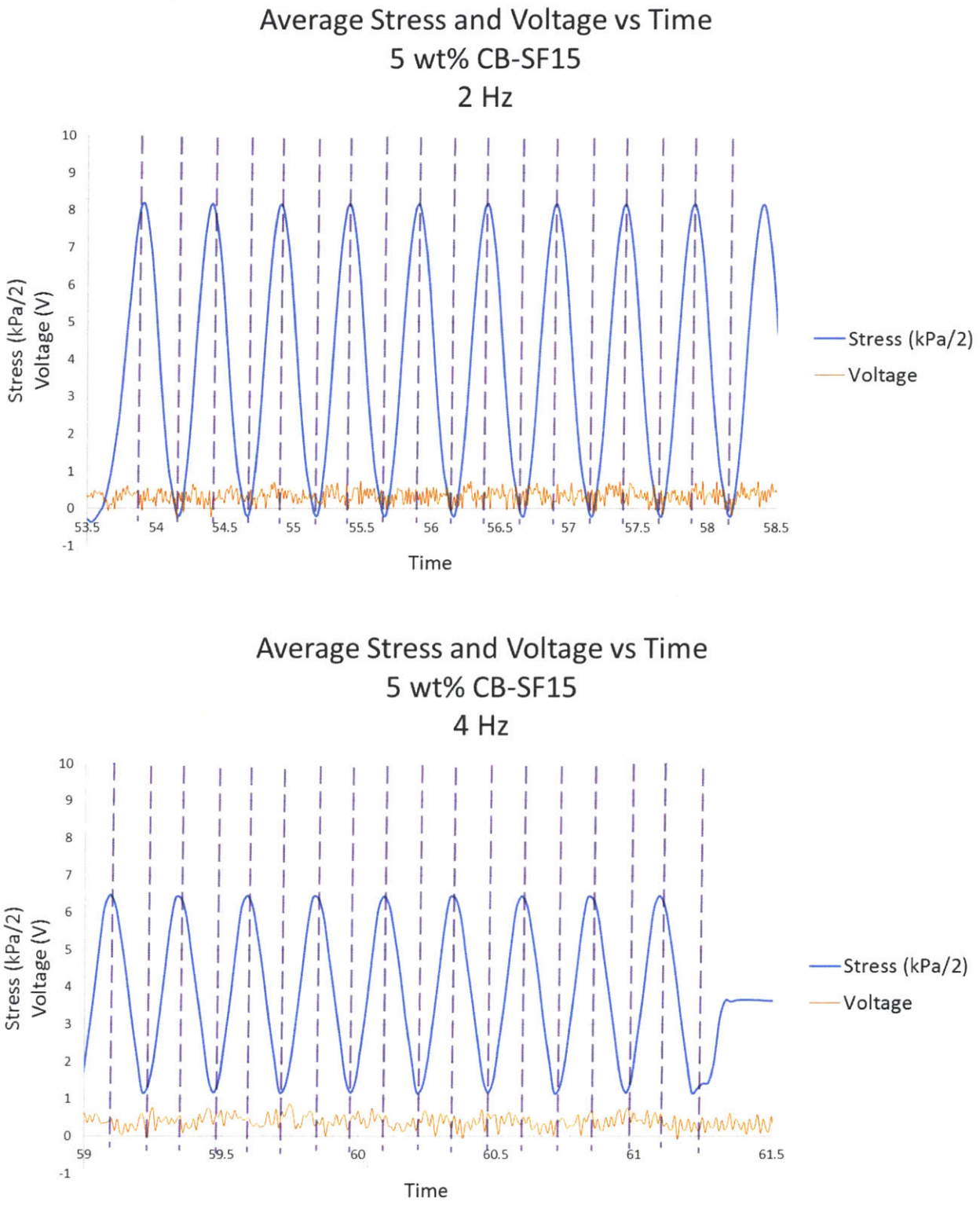

Figure 23. At 0.5 Hz, the 5 wt% samples can sense differences in pressure; however, with higher frequency, this sensitivity wanes.

5.5 wt% ratio

Ramp

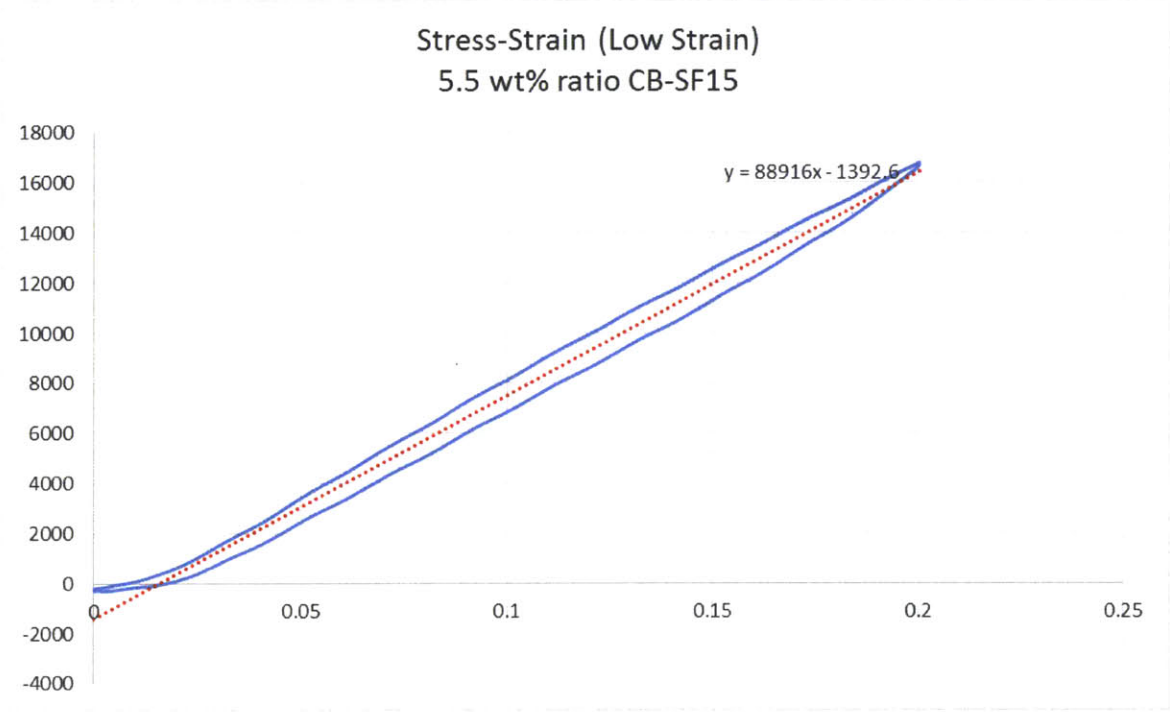

Figure 24. Compression to 5 mm, or 8%, and back down to equilibrium. Elastic modulus given by slope of fitted line.

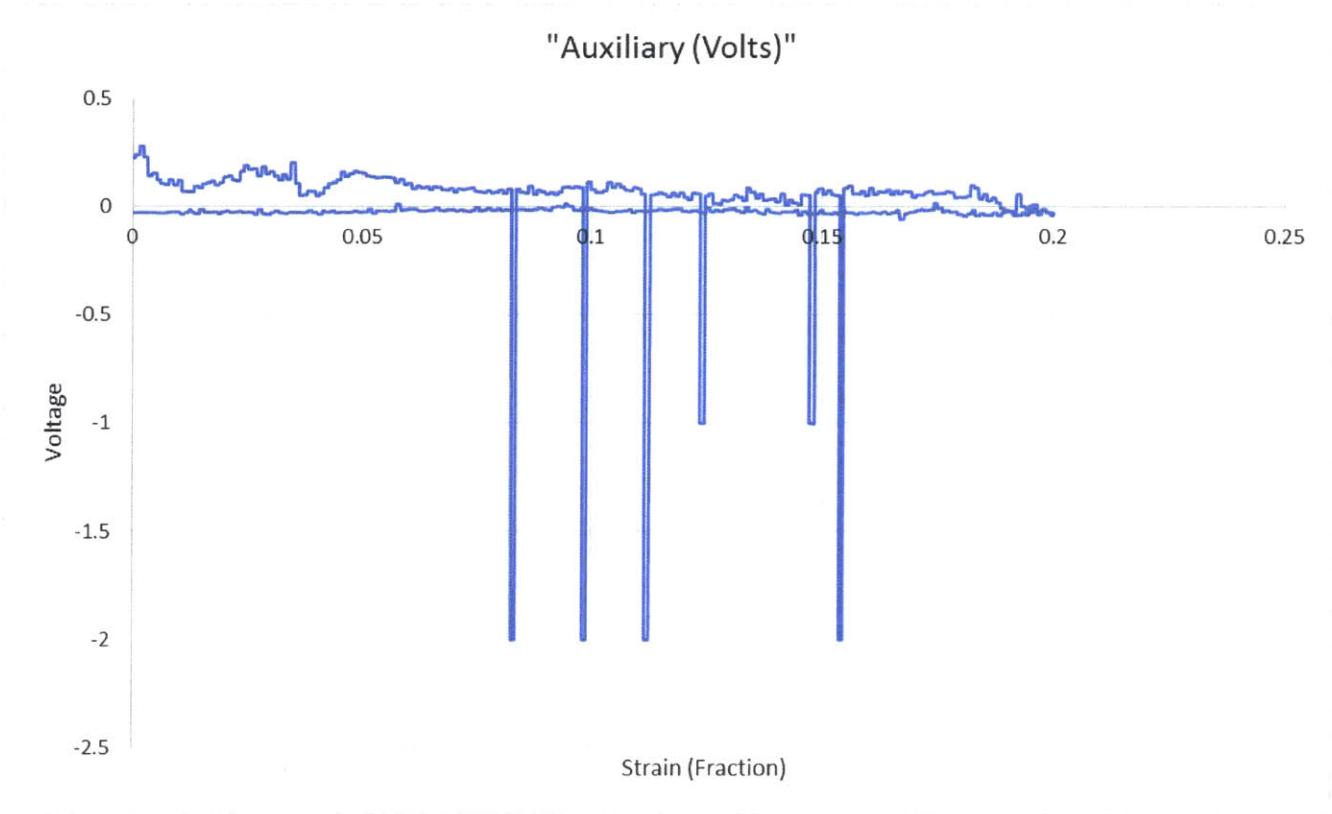

Figure 25. Hysteretic behavior is observed, with some spikes in the recorded data. These spikes occur for an unknown reason.

Sinusoidal Frequency Sweep

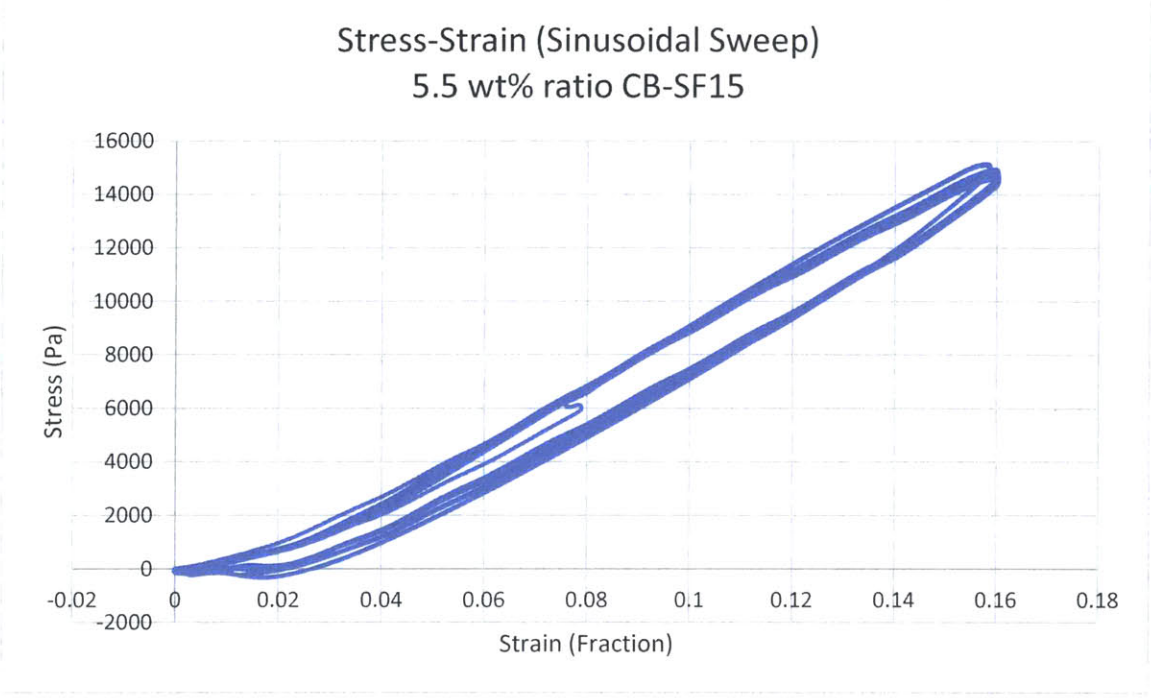

Figure 26. Frequency independence is again seen in the 5.5 wt% sample.

The 5.5 wt% material showed excellent measurable response to all frequencies tested. There seems to be unexpected behavior with a large amount of noise collected near the end of the procedure. This behavior is not seen in other samples, and may be either due to a mechanical defect in the sample composition (wiring failure, material failure, etc.) or instrumentation.

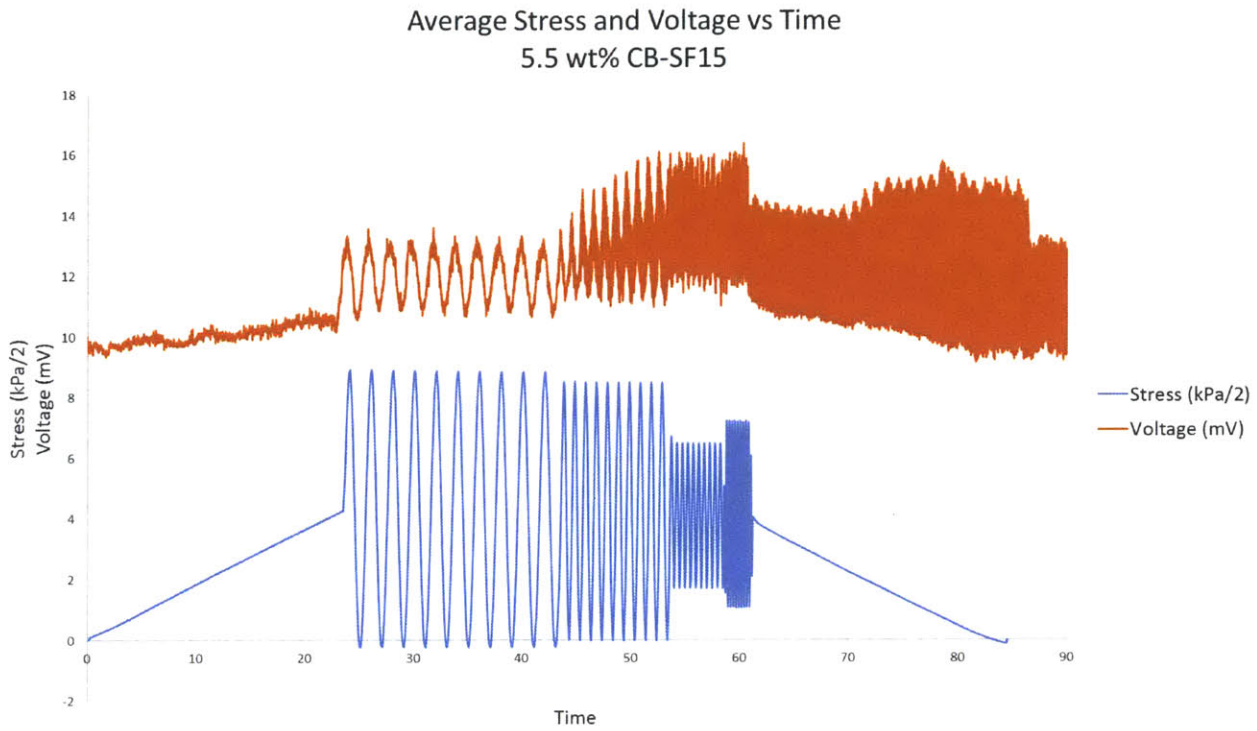

Figure 27. The entire procedure results for the 5.5 wt% samples. Strange behavior occurs at the end of the test. However, sensitivity to all frequencies can be seen.

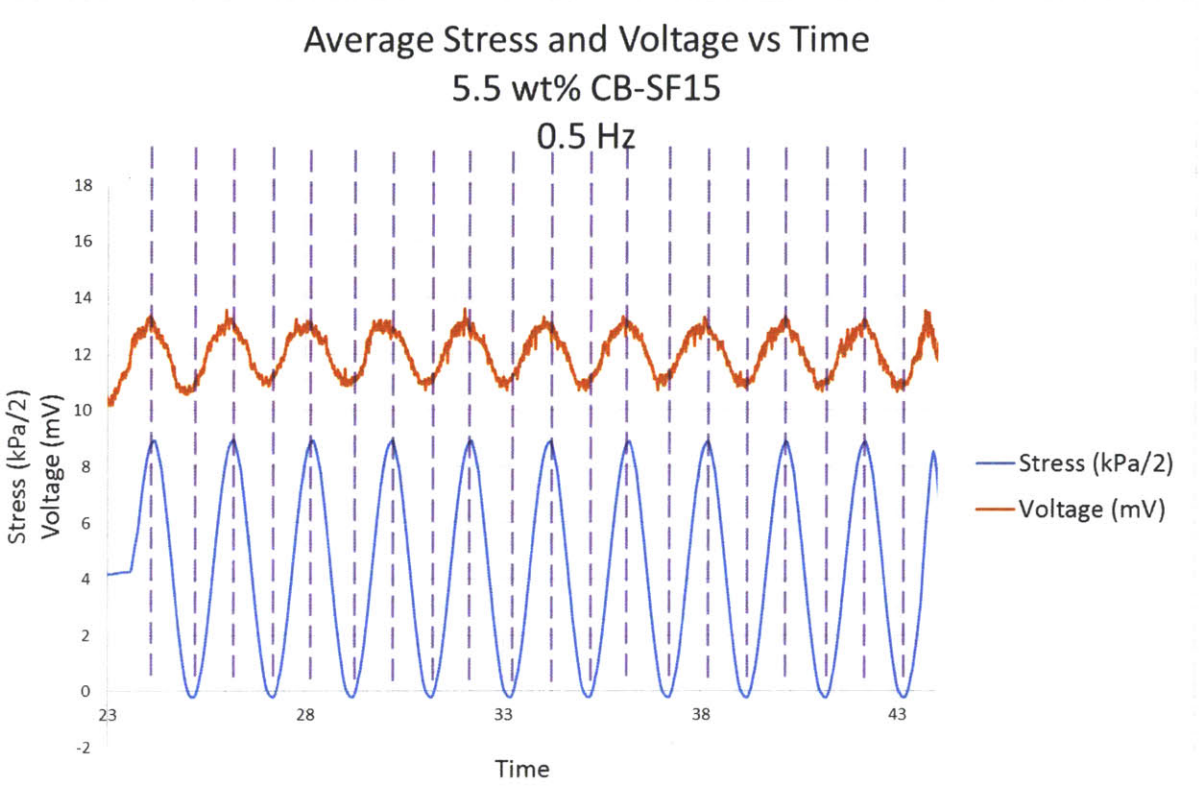
Average Stress and Voltage vs Time
5.5 wt% CB-SF15
0.5 Hz
Stress (kPa/2)
Voltage (mV)
18
16
14
12
10
8
6
4
2
0
-2
23
28
33
38
43
Time
Stress (kPa/2)
Voltage (mV)

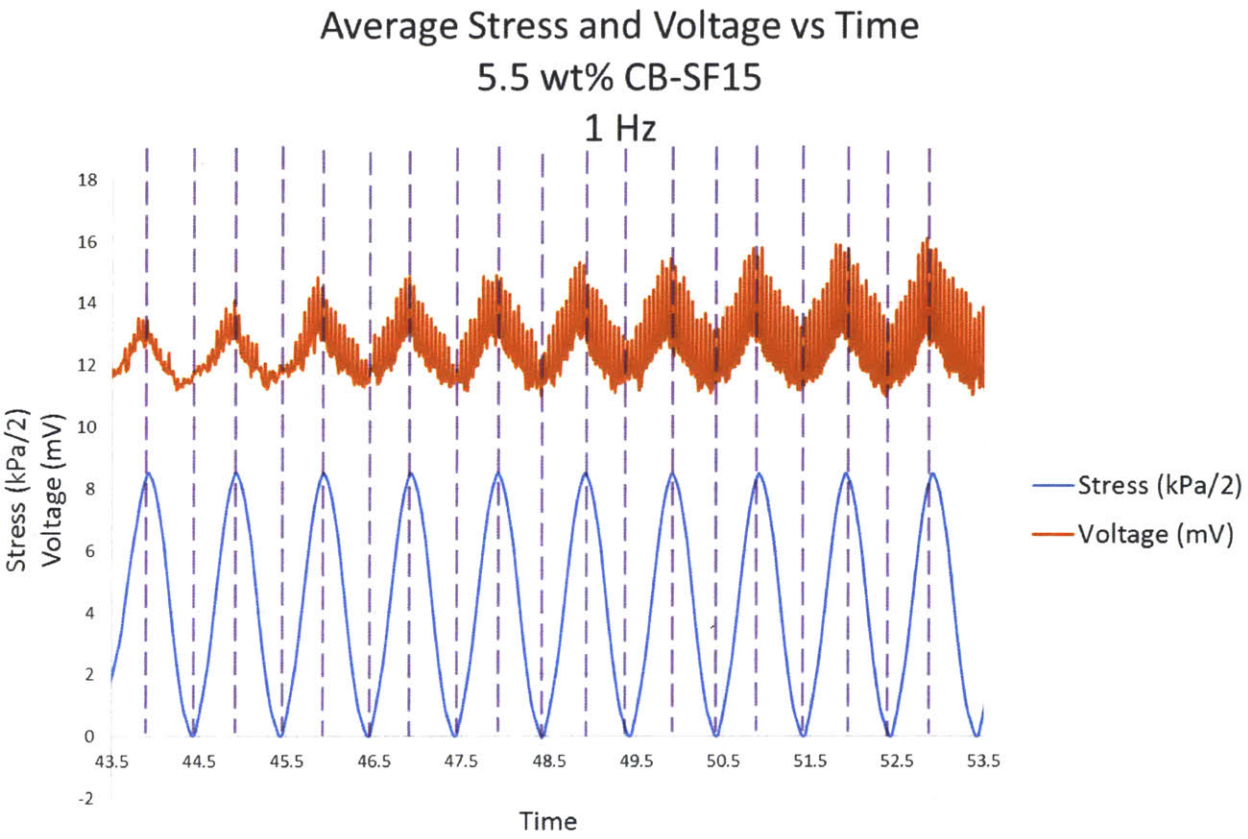
Average Stress and Voltage vs Time
5.5 wt% CB-SF15
1 Hz
Stress (kPa/2)
Voltage (mV)
18
16
14
12
10
8
6
4
2
0
-2
43.5
44.5
45.5
46.5
47.5
48.5
49.5
50.5
51.5
52.5
53.5
Time
Stress (kPa/2)
Voltage (mV)

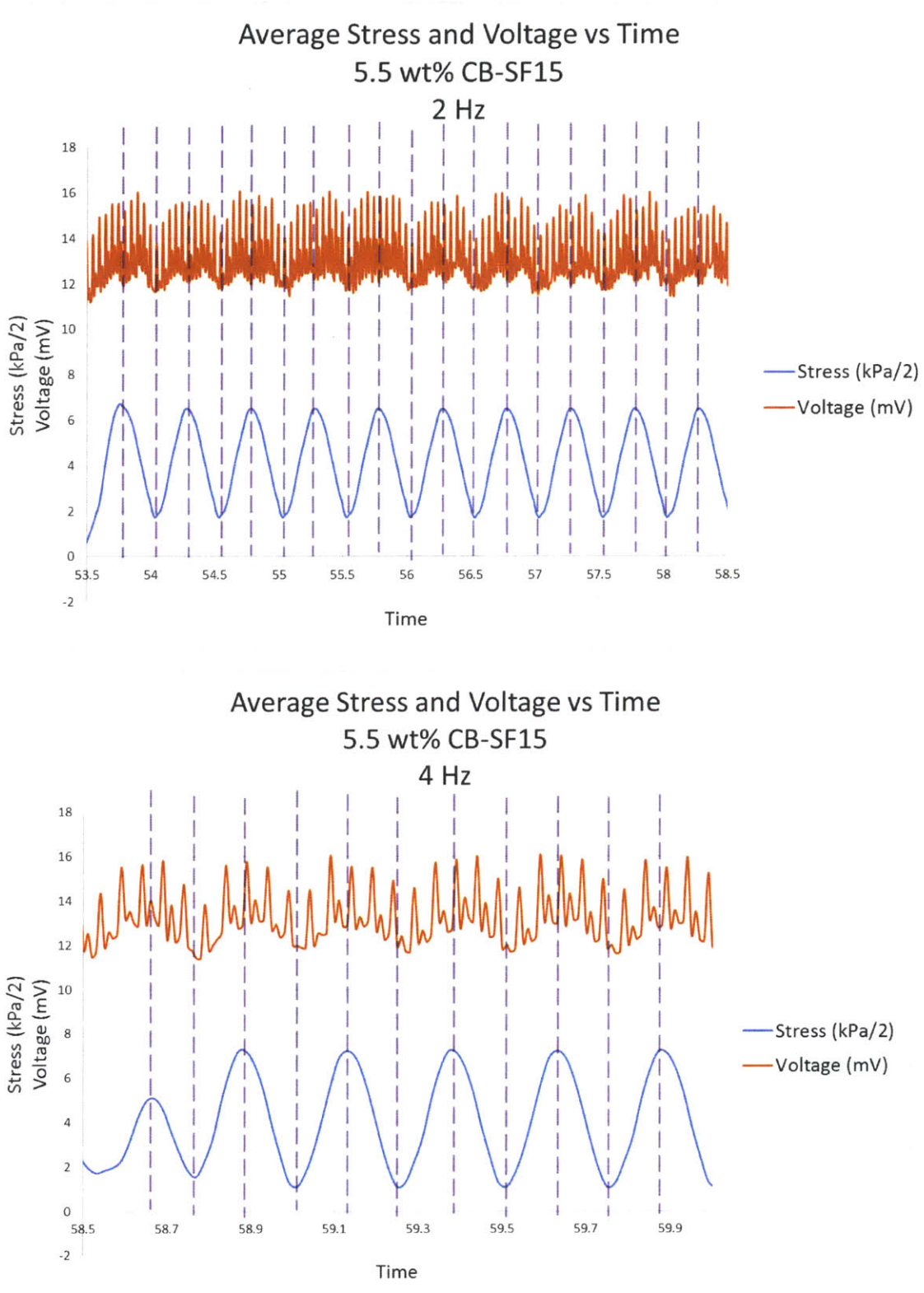

Figure 28. Sensitivity to all frequencies can be seen in the 5.5 wt% samples.

Discussion

Ramp

The ramp test was performed at a strain rate of 5 mm/min. The sample was compressed to 20% strain and then returned to 0% strain at the same rate. Hysteretic behavior is observed, and the amount of force required to strain the sample is only slightly larger when compressing than when decompressing. This is typical behavior of elastomeric materials like PDMS, and is expected behavior in the CB-PDMS foam.

Hysteretic behavior is observed in voltage response as well. Even with the large amount of noise present, the voltage observed in compression is very similar to that observed during tension, and each regime behaves similarly. Higher compression results in a higher recorded voltage.

Sinusoidal Frequency Sweep

Hysteretic behavior is clearly observed in the stress-strain plots. This test included four regimes, started from a pre-loaded condition of 20% strain: 10 cycles of 0.5 Hz frequency sinusoid of amplitude 2 mm, followed by the same number of cycles at the same magnitude for frequencies 1 Hz, 2 Hz, and 4 Hz. The frequency shows little influence on the hysteretic behavior; the material behaves similarly mechanically for all frequencies.

At 0.5 Hz frequency, the samples sense with some clarity the changes in stress and strain. However, only the 5.5 wt% was able to sense all frequencies. Further

recommendations for this material are to explore higher weight ratios of dopant in order to verify the optimum weight ratio, and to explore the limits of the magnitudes of pressure that the samples are able to detect. In addition, exploring the spectrum of frequencies open to the optimized material would provide information on the kinds of applications that this material may be useful in.

Current Explorations

Sensor arrays are being designed according to the specifications outlined in the *Materials and Methods* section, then made in order to test performance underwater. Two thicknesses of the CB-doped layer are being tested: 1/8" (thin) and 3/16" (thick). These sensors are placed on a linear stage in a water tank, where the depth to which the material is submerged can be controlled.

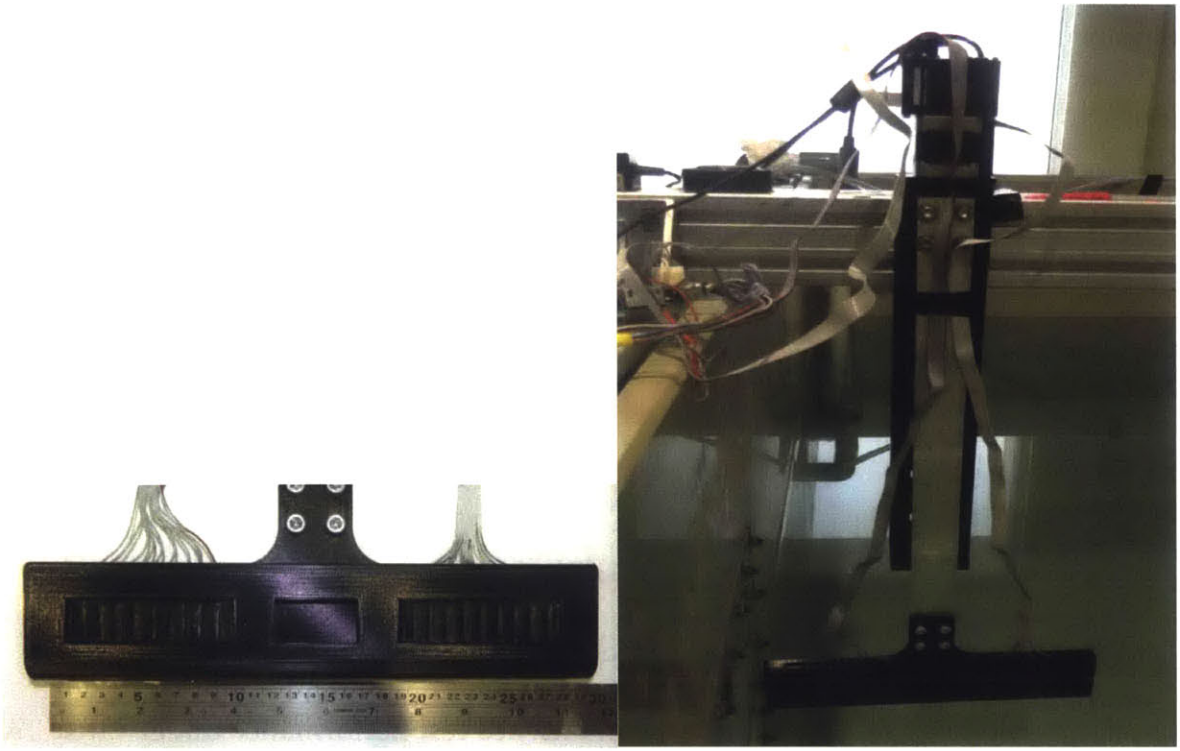

Figure 29. Underwater array sensor testing apparatus. The linear stage can be manipulated vertically, allowing the user to adjust the water pressure that the sensor is exposed to.

This sensor, placed inside of a 3D printed container leaving the foam sensing material exposed to the water without a waterproofing layer, is shown to respond to small pressures (100's of Pascals) with noticeable changes in voltage response, allowing small pressures to be sensed with confidence. Pressures near 100 Pa have been detected. This is in contrast to previous open-cell PDMS sensors, which required a waterproofing layer to be used underwater.

The sensor seems to saturate, however, at approximately 300-400 Pa (seen at the 20 second mark on the plots in Figure 30). Whether this is due to the mechanical behavior or the piezoresistive properties of the doped material is still unknown.

Optimization of this sensor array is still in progress, but shows promise as a potential lightweight, flexible sensing option for low pressure stimuli underwater.

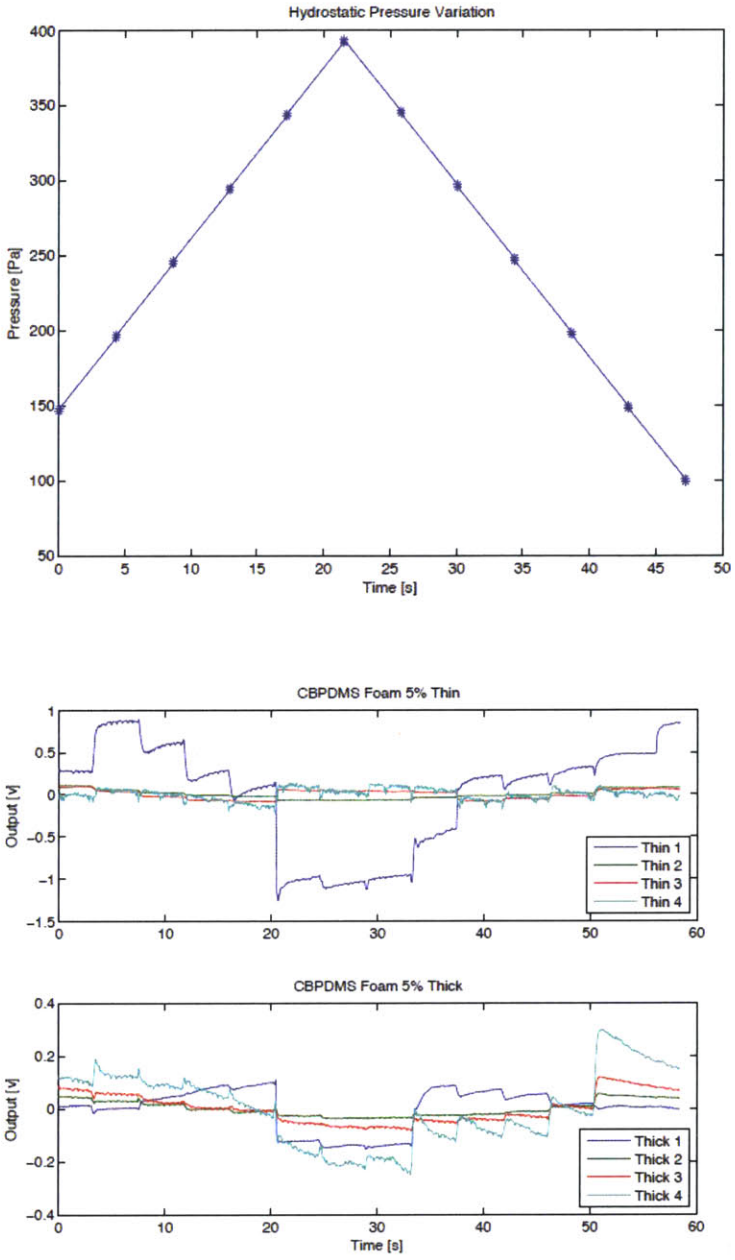

Figure 30. Results of an underwater pressure variance test. Pressure was ramped and voltage out was recorded. Data provided by Jeff Dusek, 2015.

Conclusions and Further Recommendations

This closed-cell CB-doped silicone foam has potential to be used as an underwater sensor due to its ability to sense changes in pressure with a change in resistance, and therefore a change in measured voltage output. It is flexible and elastomeric, allowing it to deform over large strains without plastic deformation. This is a useful property for a sensor that will be used over the long-term to sense fluctuations in water pressure.

Out of the concentrations studied, a 5.5 wt% ratio of CB-PDMS shows the best sensing capabilities for frequencies between 0.5 and 4 Hz. Because this was the highest concentration studied, tests involving a higher ratio of CB-PDMS should be done to verify the optimum ratio.

Difficulties in measurement in the cubic sensors might be attributed to well-recorded problems with contact resistance; this may explain the differing measurements between the sensor array and the cubic sensors. The silver-doped CB-PDMS blocks used in the array provide better contact than a wire, especially when in contact with a foam, which is composed of air-filled cells that reduce contact area.

Current work on the array sensors will provide more accurate and precise sensor results, and will show the viability of using the sensor underwater over the long-term. Further recommendations from this point include: verifying the percolation threshold in order to find the optimum weight percent ratio of CB to SF15 PDMS foam by exploring higher weight percent ratios, and testing the electric response limits of the sensor as a function of sinusoidal frequency to discover the sensor's wave-sensing capabilities, such as how strong or weak – how high or low a pressure difference – the material can sense.

Determining the lifetime of such a material is also necessary to ensure that it will survive in an underwater environment for the required span of time. Its durability in saltwater or under mechanical fatiguing will determine its feasibility for use underwater without a protective coating.

This material shows promise as a potential sensor material for underwater hydrodynamic purposes. With optimization and further exploration, it could prove a viable replacement for current acoustic and optical underwater sensing instruments.

Acknowledgements

I would like to express gratitude to Professor Jeffery Lang for his wonderful guidance and assistance throughout this project. Many thanks are due to Jeff Dusek and Matthew D'Asaro as well for the amazing amount of support received from them both. My appreciation goes to my thesis reader, Professor Bilge Yildiz, for her lovely support and assistance. I am grateful for being able to join you all in this research, knowing that there is promise to create something with such useful application and impact. Thank you for being great mentors and supporters throughout the short time we have known each other.

I would also like to thank my friends in the DMSE for supporting me in this project: Joanna Chen, JJ Hernandez – you are such wonderful friends and classmates, and I am honored to have been able to enjoy this time together with you. My gratitude extends to the entire 2015 Course 3 class; it was a tremendous joy to study with you all.

To my friends outside of my department as well – to Simmons Hall and its residents; to the Baptist Student Fellowship; to Professor John Belcher; to Stephanie Chen, my longtime roommate; to Nadiah Jenkins, my longtime neighbor – I could not have come this far this without your love and support.

I would like to thank my family for their unending devotion and love overflowing. You are all some of my best friends in the world, and I love you all so dearly. I could not have accomplished an MIT degree without you all, but more importantly, I would not be who I am today without your love, support, guidance, and friendship.

I thank God for the opportunity to have been able to study here at MIT for four years, for the opportunity to graduate an engineer and a scientist, to be able to make such wonderful and brilliant friends, and to be able to grow mentally and spiritually.

Thank you all for your support throughout this project and throughout the last four years at the Institute. I could not have done it without you all – I give my many, many thanks, and my warmest wishes for your futures.

This thesis was partially supported by the Center for Sensorimotor Neural Engineering through an ERC Grant from the U.S. National Science Foundation.

Bibliography

1. Crimmins, D.; Manley, J. NOAA Ocean Explorer. What Are AUVs, and Why Do We Use Them? http://oceanexplorer.noaa.gov/explorations/08auvfest/background/auvs/auvs.html. (accessed April 23, 2015).

2. Yaul, F. M.; Bulovic, V.; Lang, J. H. A Flexible Underwater Pressure Sensor Array Using a Conductive Elastomer Strain Gauge. Journal of Microelectromechanical Systems 2012, 21, 897–907.

3. Montgomery, J. C.; Coombs, S.; Baker, C. F. The Mechanosensory Lateral Line System of the Hypogean form of Astyanax Fasciatus. Environmental Biology of Fishes 2001, 62, 87–96.

4. Naeem, W.; Sutton, R.; Ahmad, S. M.; Burns, R. S. A Review of Guidance Laws Applicable to Unmanned Underwater Vehicles. Journal of Navigation 2003, 56, 15–29.

5. Schrope, M. Whale deaths caused by US Navy's sonar. *Nature* **2002**, *415*, 106.

6. Dusek, J.; Kottapalli, A.; Woo, M.; Asadnia, M. et al.; Development and testing of bio-inspired microelectromechanical pressure sensor arrays for increased situational awareness for marine vehicles. Smart Mater. Struct. 22 (2013) 014002 (13pp) doi:10.1088/0964-1726/22/1/014002. (accessed April 27, 2015)

7. Bleckmann, H. Role of the Lateral Line in Fish Behavior. In The Behavior of Teleost Fishes; Pitcher, T., Ed.; Springer US, 1986; p 177.

8. Kottapalli AG, Asadnia M, Miao J, Triantafyllou M. Touch at a distance sensing: lateral-line inspired MEMS flow sensors. Bioinspir Biomim. 2014 Dec;9(4):1-14. PubMed PMID: 25381677.

9. Woo, M. Development of a Porous Piezoresistive Material and its Applications to Underwater Pressure Sensors and Tactile Sensors. Masters Thesis, Massachusetts Institute of Technology, Cambridge, MA, 2013.

10. Y. Ishigure, S. Iijima, H. Ito, T. Ota, H. Unuma, M. Takahashi, Y. Hikichi, H. Suzuki. Electrical and elastic properties of conductor-polymer composites. The Journal of Materials Science, 19990615, Volume 34, Issue 12, pp 2979-2985. doi:10.1023/A:1004664225015. (accessed March 10, 2015)

11. TDA Research. Specialty Composites. http://www.tda.com/eMatls/composites.htm. (accessed April 20, 2015)

12 Sotta, P.; Long, D. The crossover from 2D to 3D percolation: theory and numerical simulations. Eur Phys J E Soft Matter. 2003 Aug;11(4):375-87. PMID: 15011103.

13. Yoshizawa, M., Jeffery, W. R., van Netten, S. M., McHenry, M. J. The sensitivity of lateral line receptors and their role in the behavior of Mexican blind cavefish (Astyanax mexicanus). The Journal of Experimental Biology, 217(6), 886–895. 2014. doi:10.1242/jeb.094599. (accessed April 20, 2015)

Appendix

Mathematica Code for Calculation of Approx. Percolation Threshold

The percolation threshold was calculated using a rough model of the cell wall as a slab. Measurements for the dimensions of the hypothetical slab were taken from cell wall average thicknesses at various points along the wall, and measurements were taken from various walls.

The amount of mass of Carbon Black needed for a specific volume of foam was calculated using the relative density of the foam and the approximate percolation threshold for a slab (0.3 volume fraction). Using the size of the Carbon Black particles and its density, the weight percent required to reach 0.3 volume fraction Carbon Black was calculated. This number was calculated to be approximately 0.64 g, or 6.4% for a 10 g, 2.5 cm long cube of CB-SF15 foam.

The calculation in Wolfram Mathematica software is given:

In[146]:= foamreldensity = ((2 g / (0.025 * 0.025 * 0.005 m^3)) / (3.93 g / (0.015^3 m^3)))

Out[146]= 0.549618

In[169]:= 0.30 (0.165 / 2 mm * 0.464 / 2 mm * 0.464 / 2 mm) 10^-9 m^3 / mm^3

Out[169]= 1.33214 × 10^-12 m^3

In[170]:= 1.33 × 10^-12 m^3 / ((4/3) Pi (2.1 × 10^-8 m)^3)

Out[170]= 3.42851 × 10^10

In[163]:= gpp = ((4/3) Pi (2.1 × 10^-8 m)^3) 2 × 10^6 g / m^3

Out[163]= 7.75848 × 10^-17 g

In[171]:= percthreshdensity = gpp * 3.42 × 10^10 / (0.0355 × 10^-9 m^3)

Out[171]= 74743.6 g / m^3

In[172]:= ptdfoam = percthreshdensity * foamreldensity

Out[172]= 41080.5 g / m^3

In[173]:= ptdfoam * (0.025 m)^3

Out[173]= 0.641882 g